GG 711: Advanced Techniques in Geophysics and Materials Science

Optical Microscopy: Lecture 5

Confocal Raman Microscope

Application of Raman Spectroscopy in Geophysics and Materials Science

Pavel Zinin

HIGP, University of Hawaii, Honolulu, USA

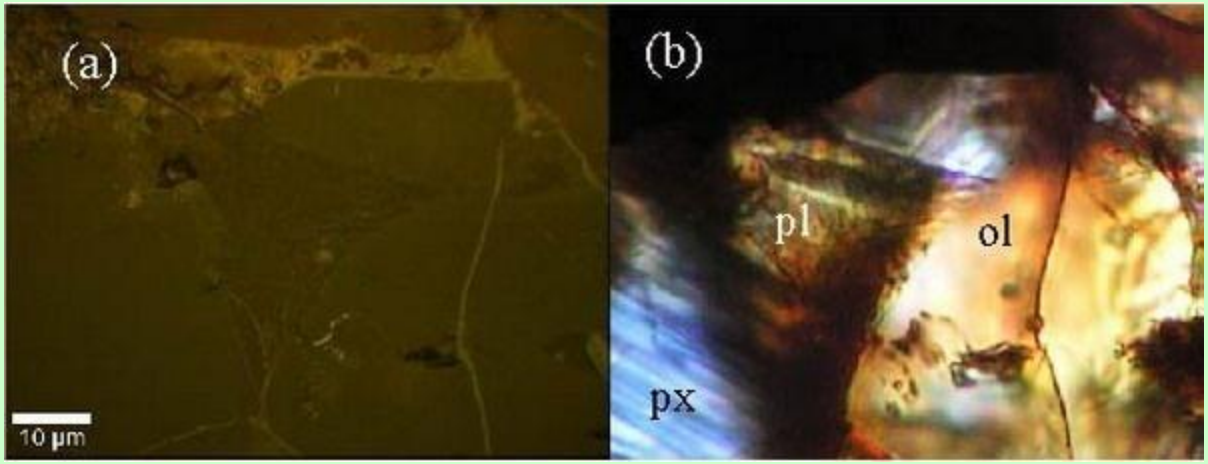

www.soest.hawaii.edu\~zinin

Confocal Microscopy

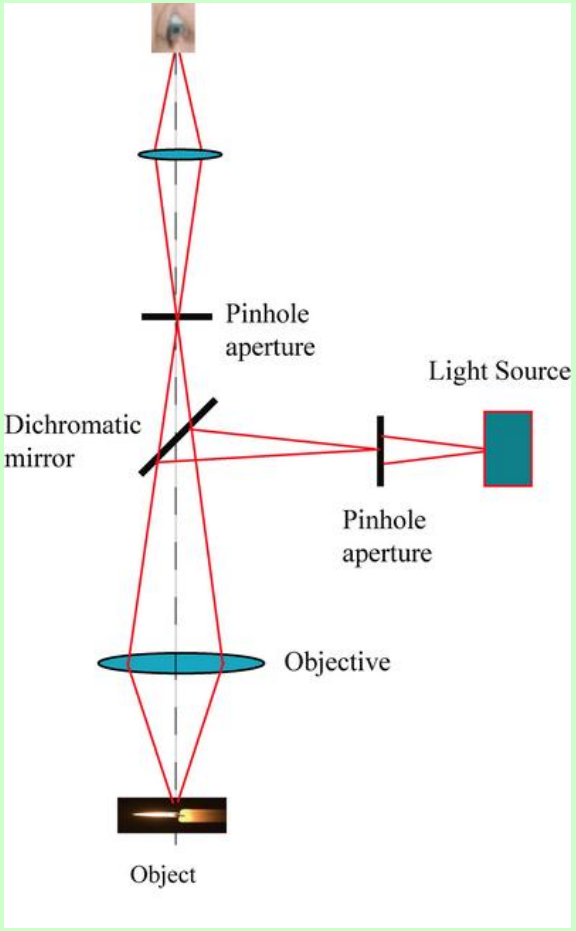

Confocal Optical Microscope

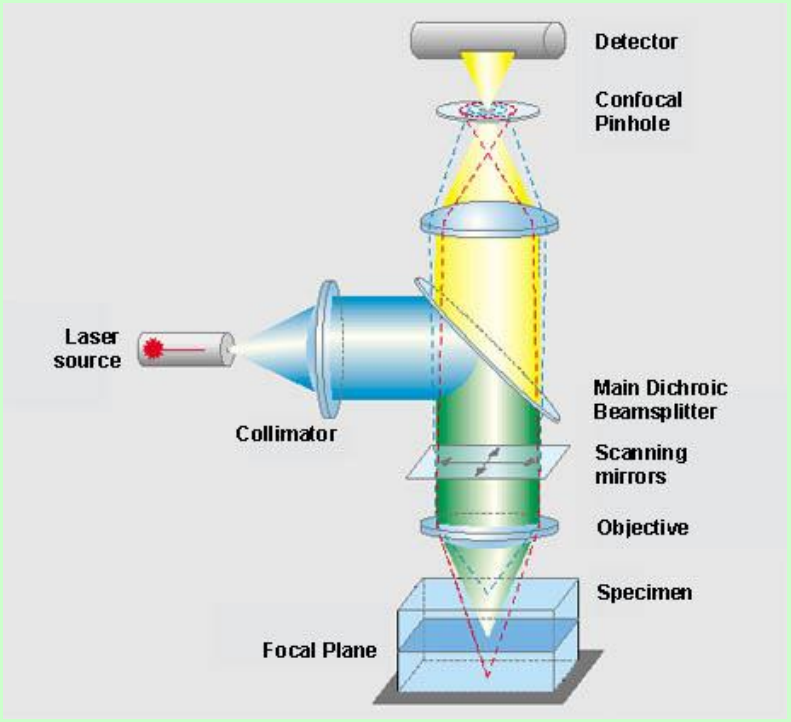

Confocal Laser Optical Microscope

Confocal Raman Microscope

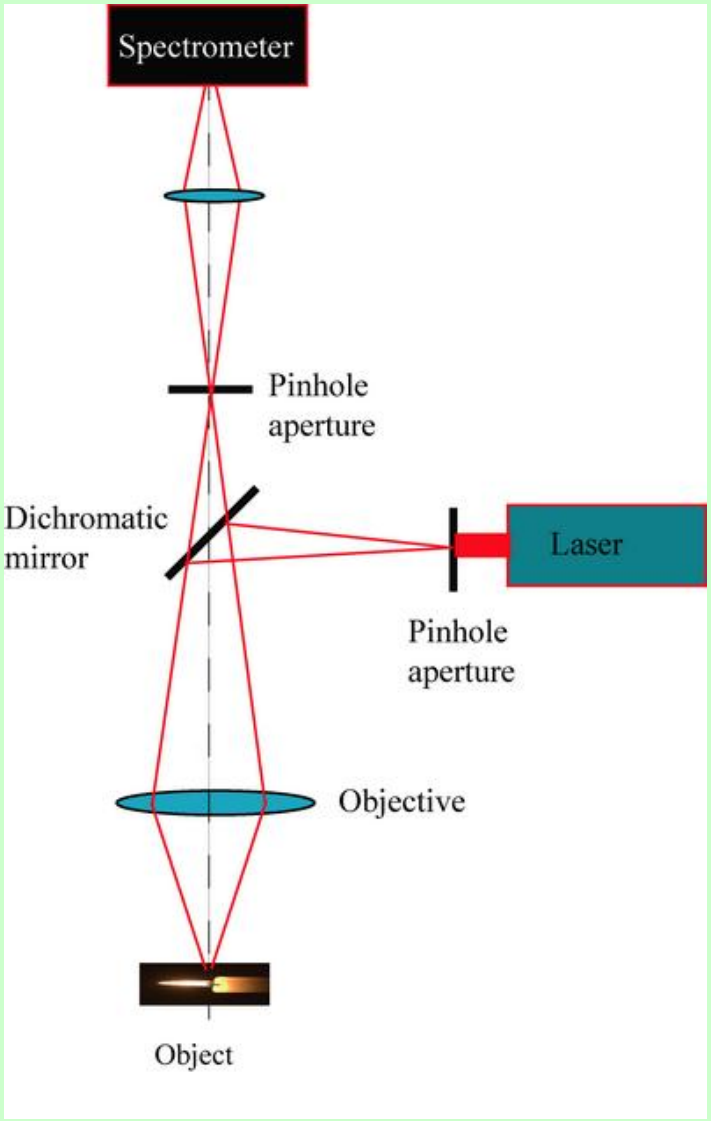

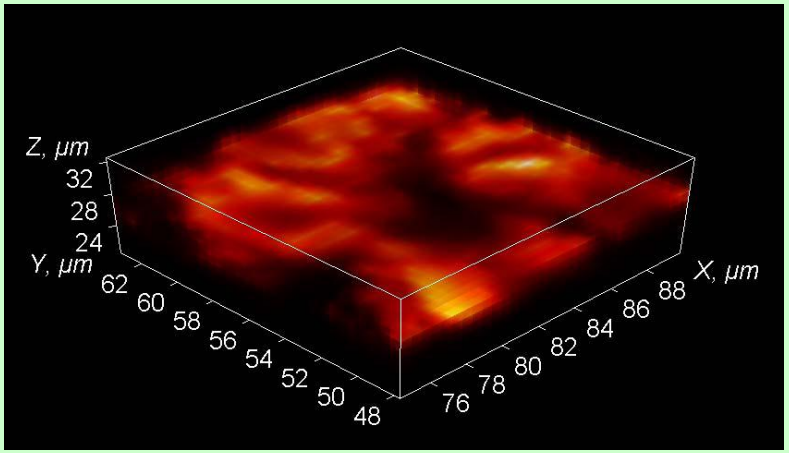

3D Intensity Distribution at peak ~600 cm-1 from normal material LiCoO2 (From Nanofinder)

Scattering of Light –Energy Diagram

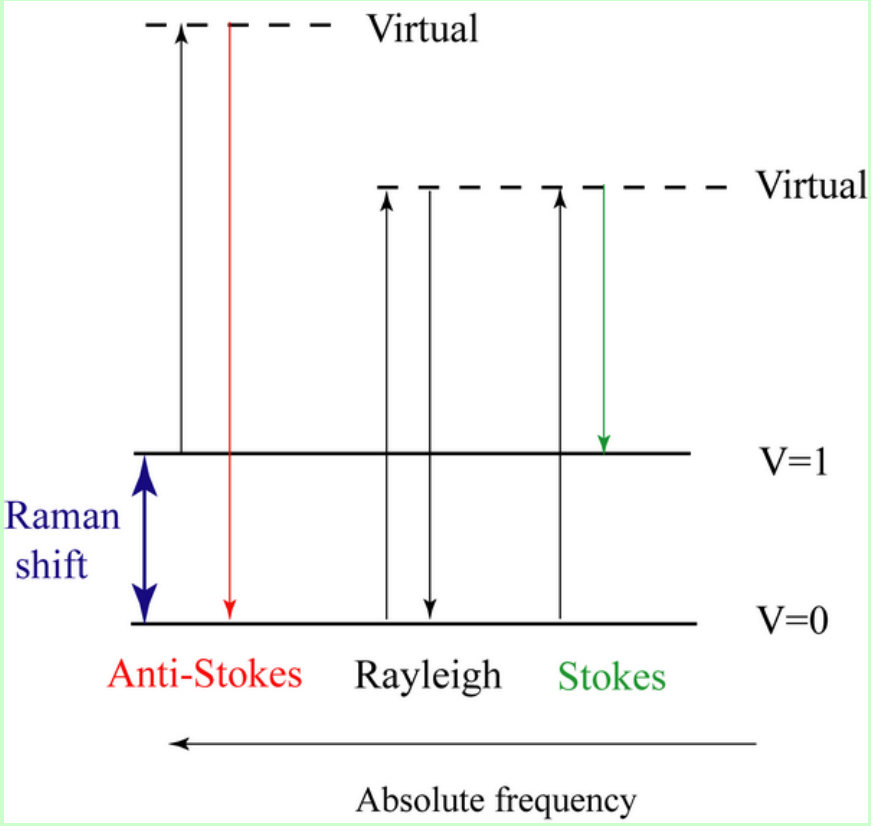

It is also useful to describe Raman scattering in terms of the discrete vibrational energy states of each molecular vibrational mode. This is commonly done by considering a vibrational energy, where the discrete vibrational states each correspond to the vibrational quantum numbers

For a population of molecules with the ground vibrational state (j=0) heavily favored at low to moderate temperatures. It is noted that molecules in upper vibrational quantum states (e.g. V = 1) still vibrate at the fundamental frequency V_{vib}, although the probability of finding the atoms displaced about their equilibrium position changes.

Raman scattering may be interpreted as a shift in vibrational energy state due to the interaction of an incident photon. The incident EM wave induces an oscillating dipole moment thereby putting the molecular system into a virtual energy state. The energy level of the virtual state is generally much greater than the vibrational quanta, but is not necessarily (and generally not) equal to any particular electronic

Raman-Mandelstam Scattering

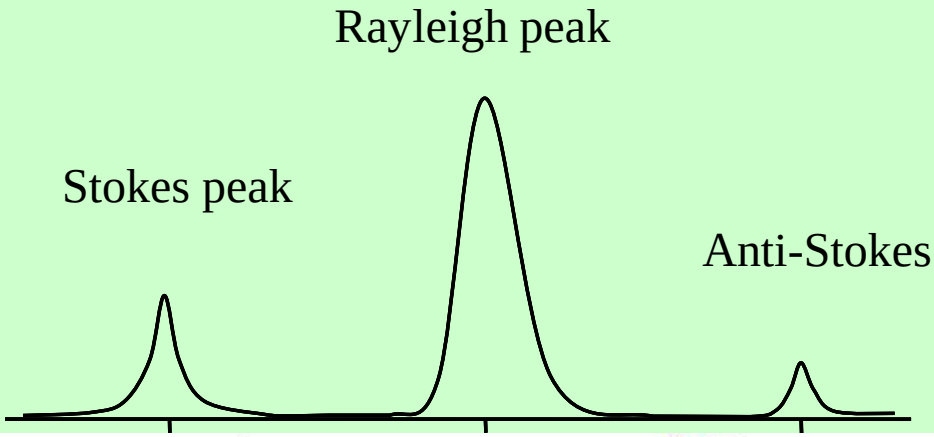

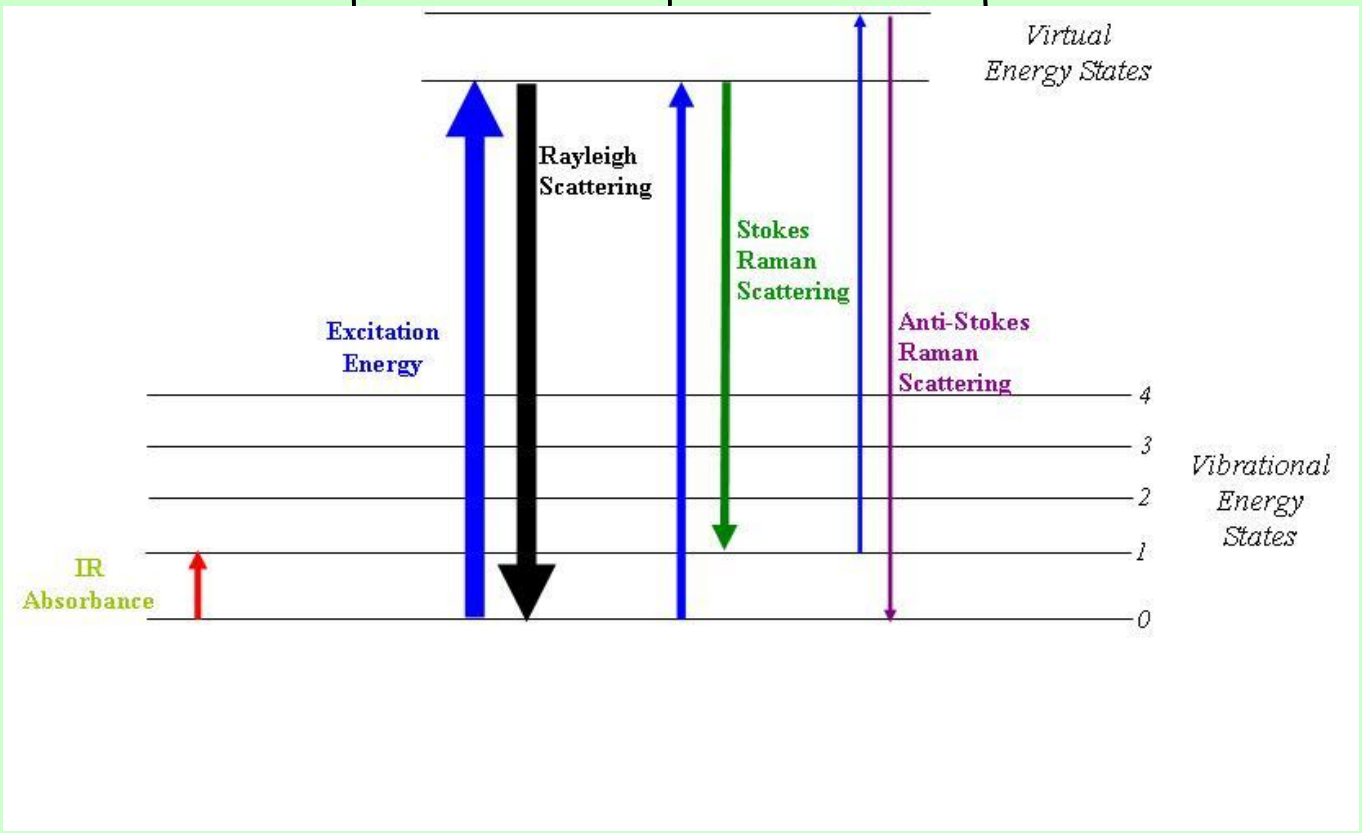

3D Raman image of polystyrene beads

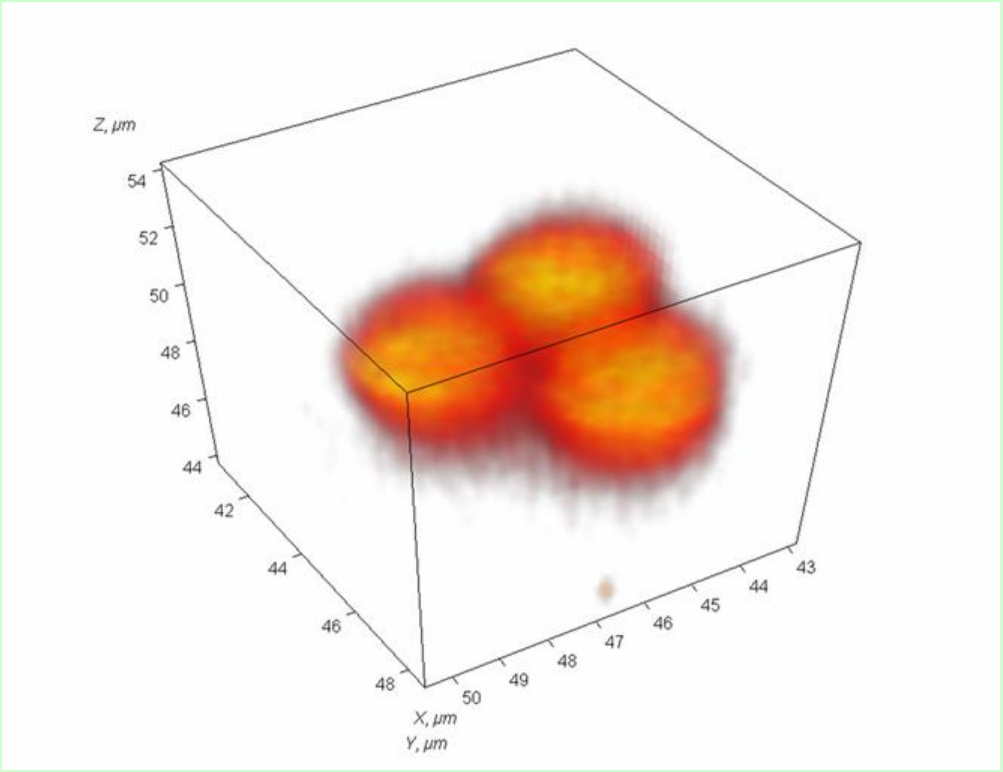

3D Raman image of Polystyrene beads
(at 1000 cm^{-1} peak intensity)

Resolution : 32 x 32 x 15 points, 250 x 250 x750 nm step
Measuring time : 90 min
Mapping speed : 0.3 sec/point
Laser : 532 nm, 1 mW (on sample)

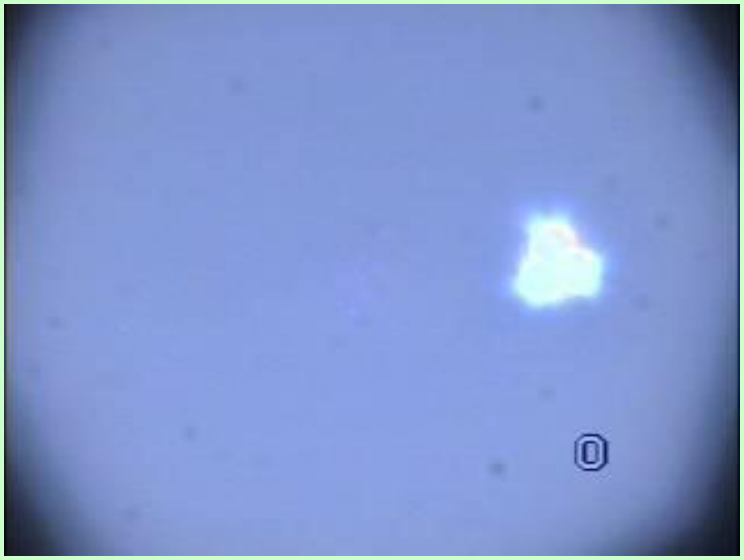

Optical Image

From Nanofinder, Flex, 2010

Raman Spectroscopic Study of Roosevelt County (RC) 075 Chondrite

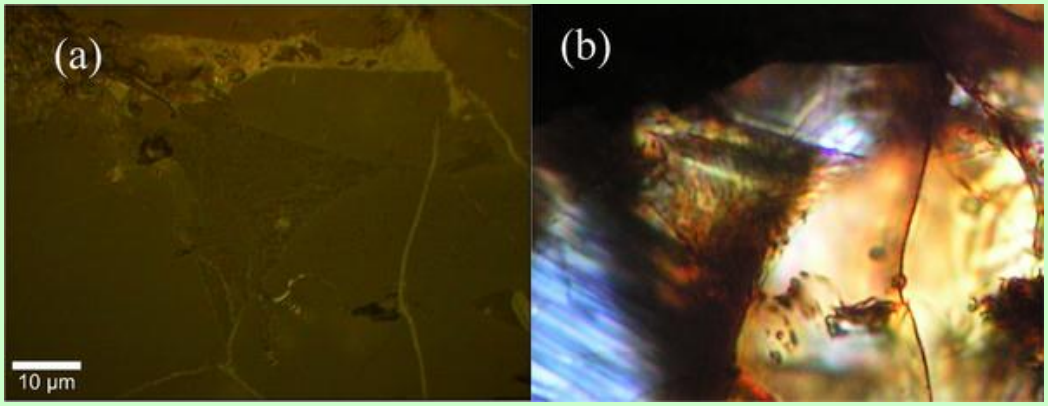

Reflected (a) and cross polarized transmitted (b) light images of RC 05.

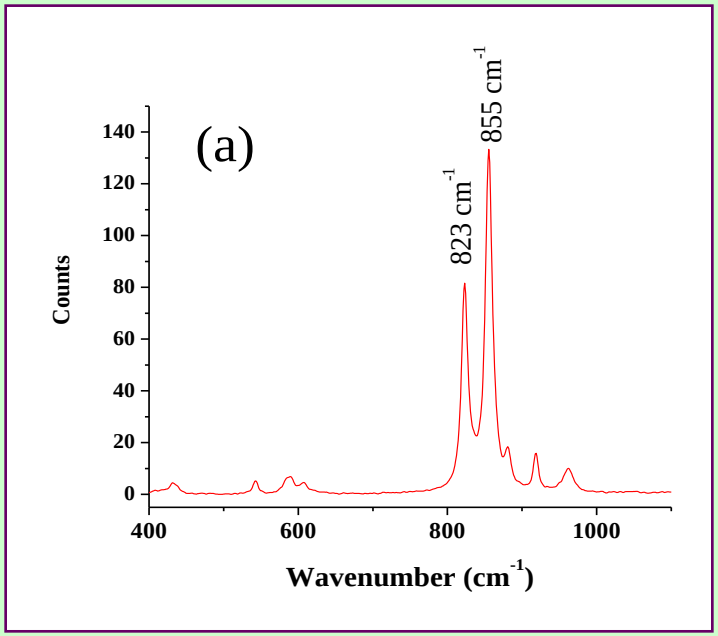

Raman spectrum of olivine (a) and map of the Raman peak centered at 855 cm^{-1} (b). The intensity of the 855 cm^{-1} peak is shown in a green color scale

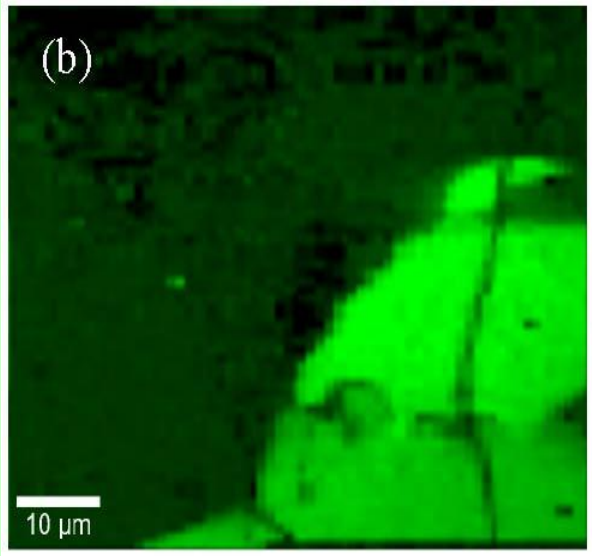

Raman Spectroscopic Study of Roosevelt County (RC) 075 Chondrite

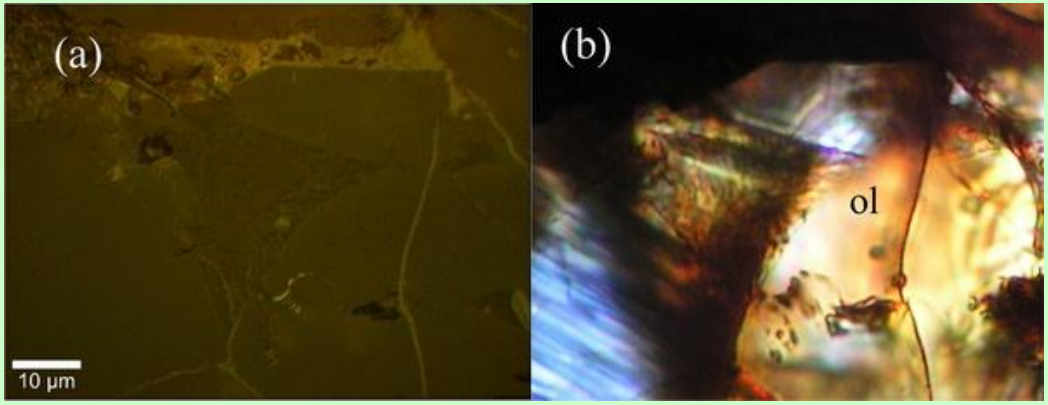

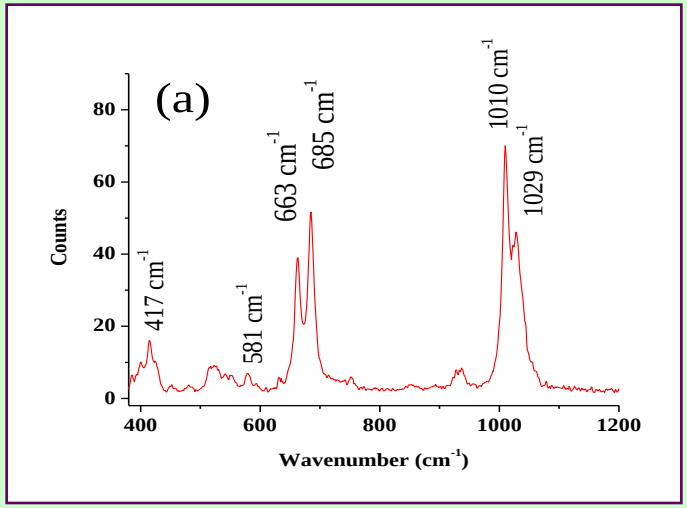

Reflected (a) and cross polarized transmitted (b) light images of RC 05: *ol* = olivine;.

Raman spectrum of the clinoenstatite (a) and map of the Raman peak centered at 1010 cm^{-1} (b). The intensity of the 1010 cm^{-1} peak is shown in a yellow color scale

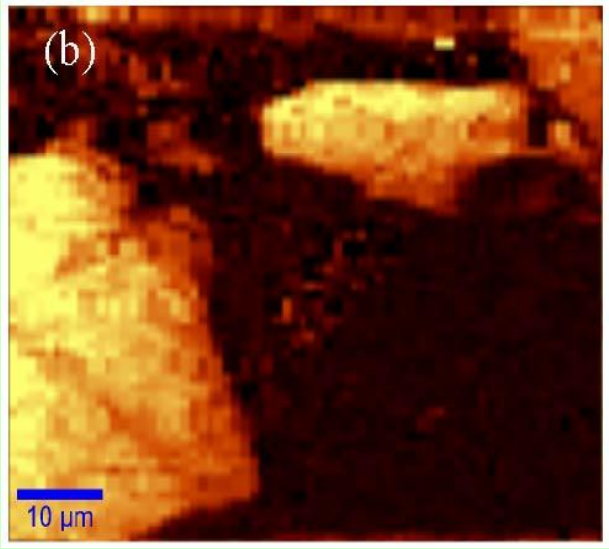

Raman Spectroscopic Study of Roosevelt County (RC) 075 Chondrite

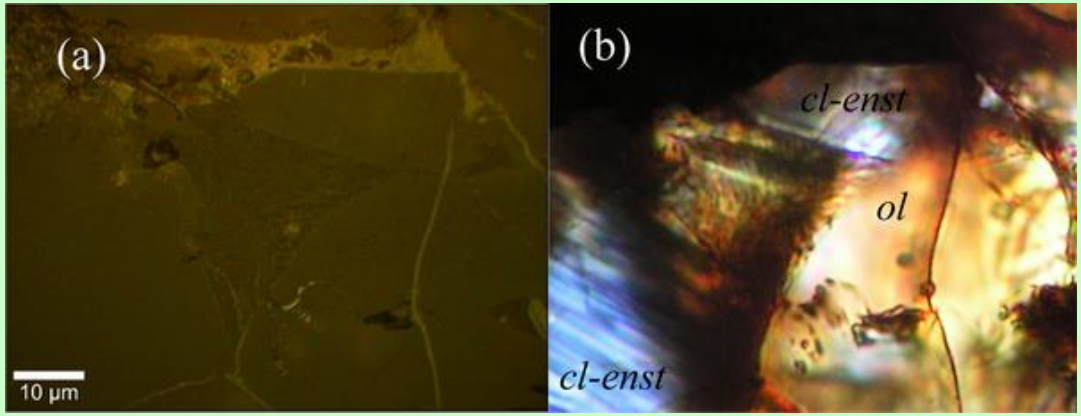

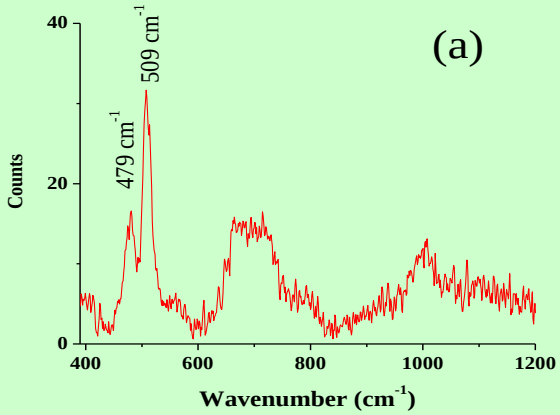

Reflected (a) and cross polarized transmitted (b) light images of RC 05: *ol* = olivine; *cl-enst* = clinoenstatite.

Raman spectrum of the plagioclase (a) and map of the Raman peak centered at 509 cm^{-1} (b). The intensity of the 509 cm^{-1} peak is shown in a blue color scale.

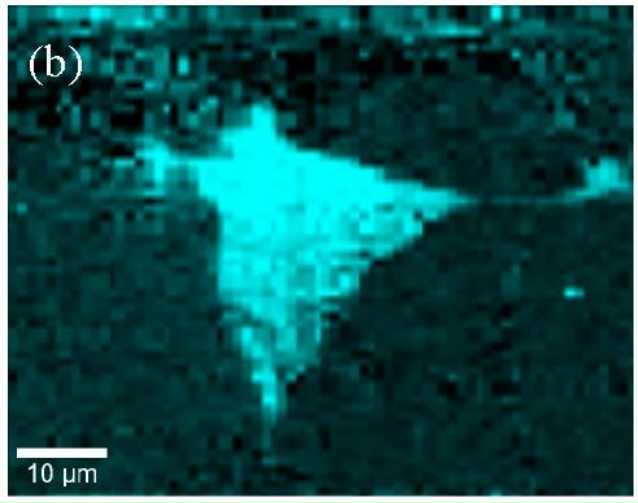

Optical images of yeast cells

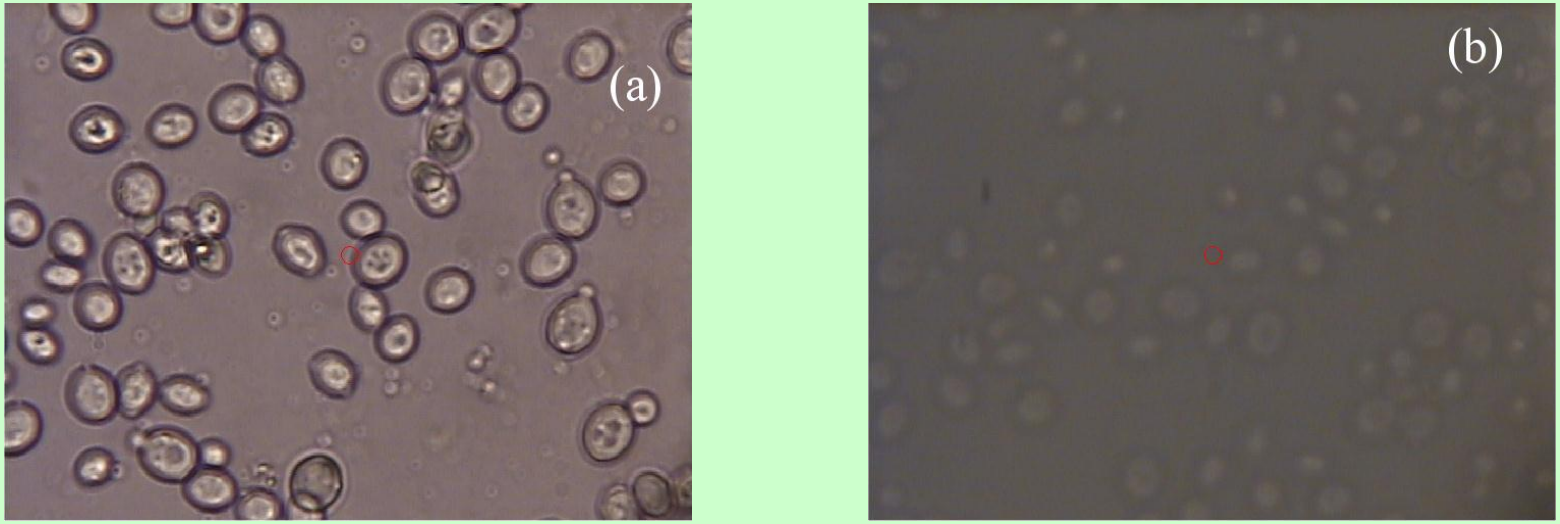

Optical images of yeast cells on glass (100x objective) in transmission mode (a), in reflection mode (b). The red circles mark the position of the laser beam.

Optical images of yeast cells

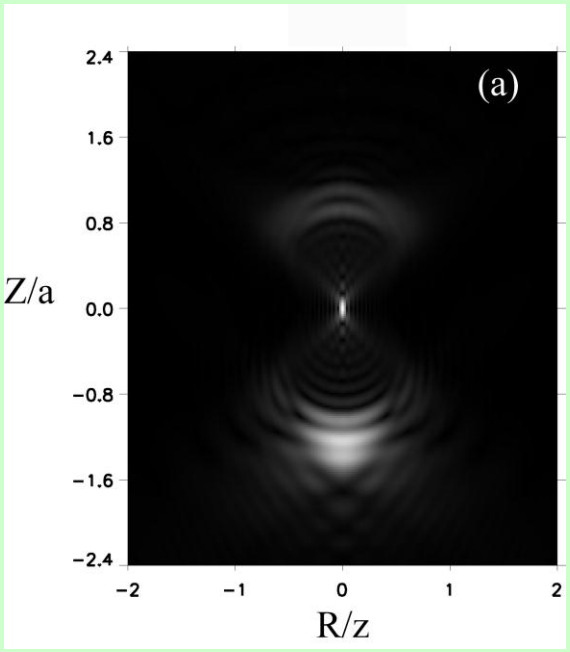

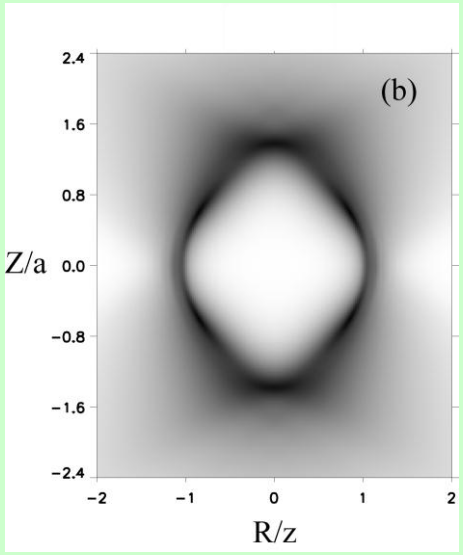

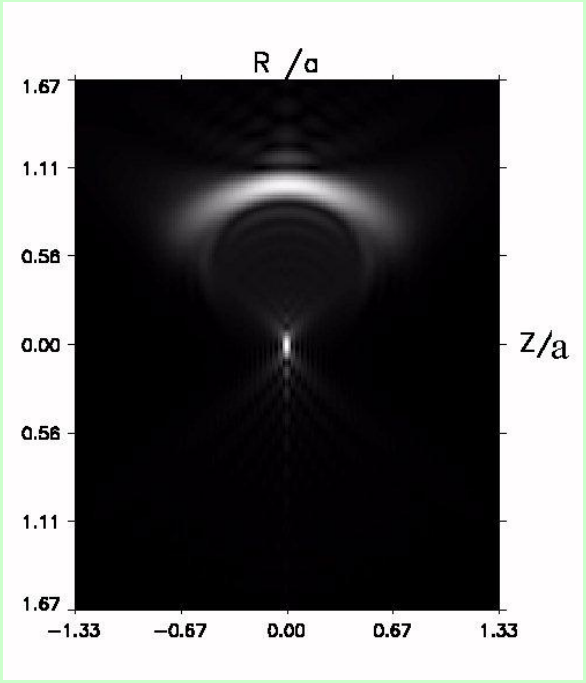

Calculated vertical scans through a transparent sphere with refraction index of 1.05 and refraction index of surrounding liquid of 1.33: (a) reflection microscope with aperture angle 30 o; (a) transmission microscope with aperture angle 30^{o}.

Optical images of yeast cells

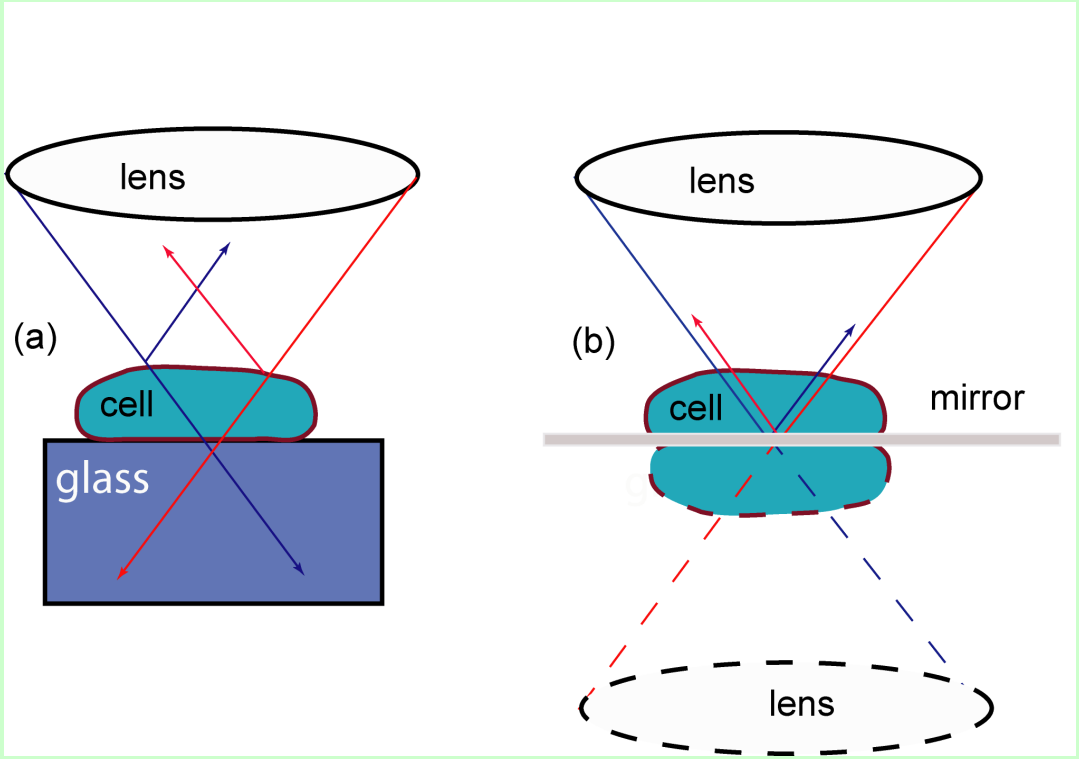

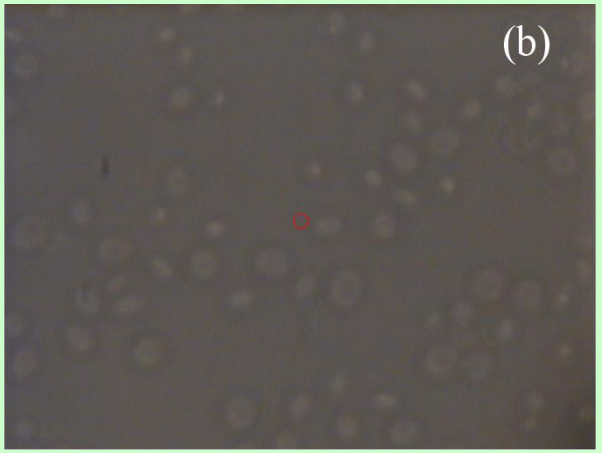

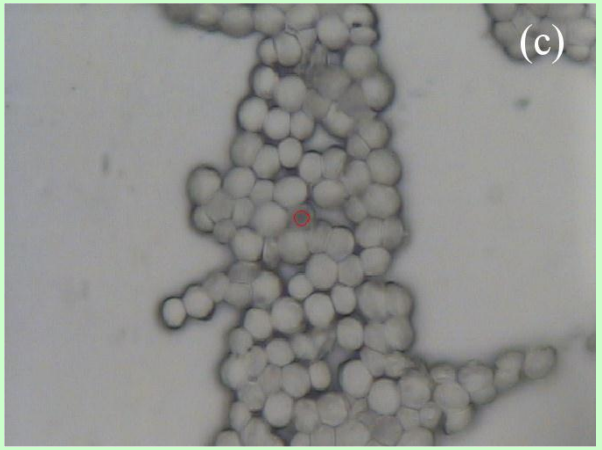

Sketch of the optical rays when cell is (a) attached to the glass substrate or (b) to mirror.

Emulated Transmission Confocal Raman Microscopy

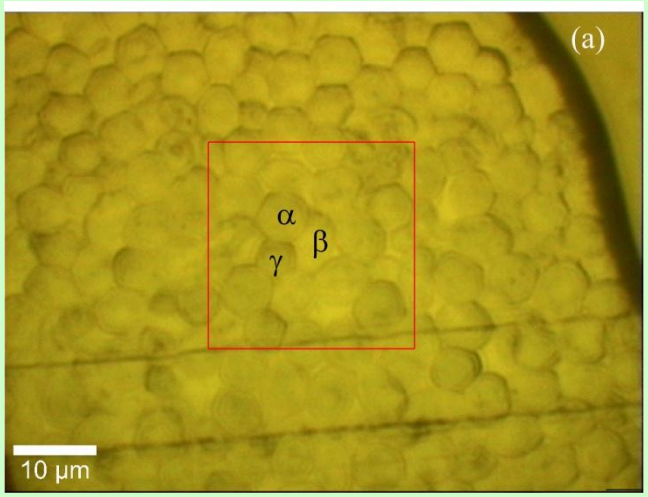

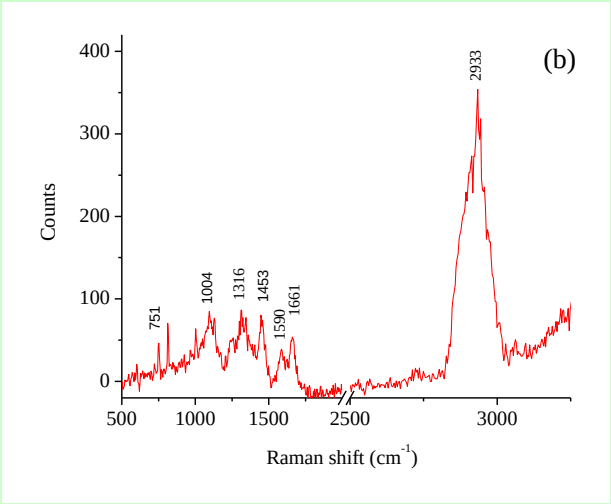

Optical image of the yeast bakery cells in the reflection confocal microscope. Rectangle shows the area of the Raman mapping. (a) Raman spectra of the cell α measured with green laser excitation (532 nm, WiTec system).

Map of the Raman peak intensity centered at 2933 cm-1. The intensity of the 2933 cm-1 peak is shown in a yellow color scale. (b) Map of the Raman peak intensity centered at 1590 cm-1. The intensity of the 1590 cm-1 peak is shown in a green color scale.

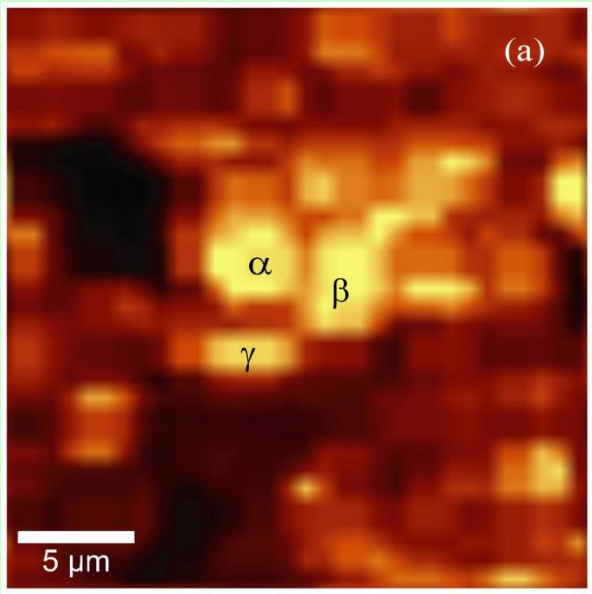

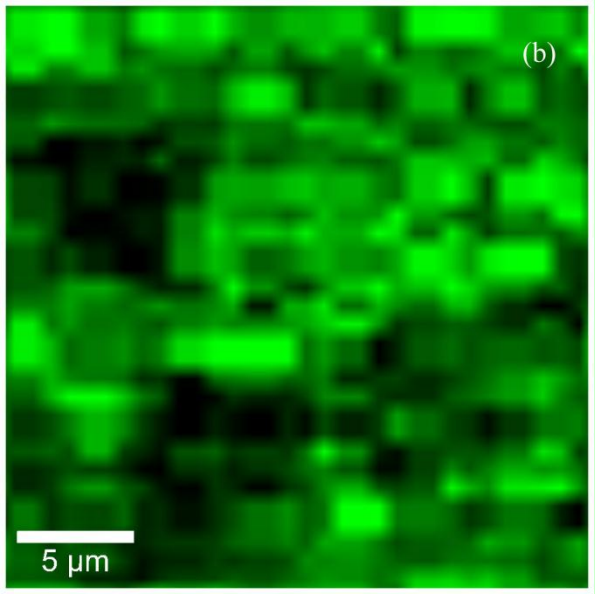

Raman Spectroscopy of Carbon Materials

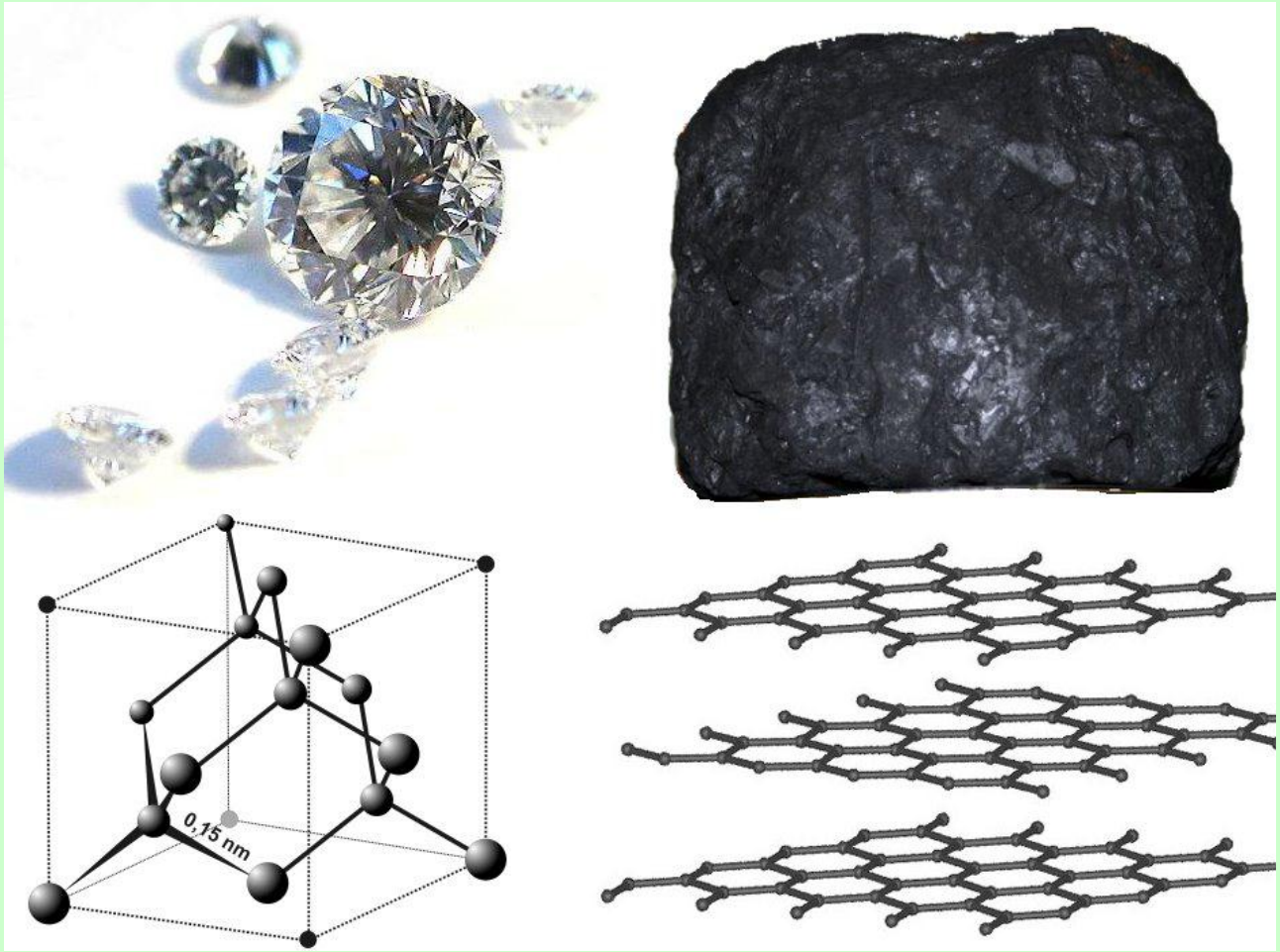

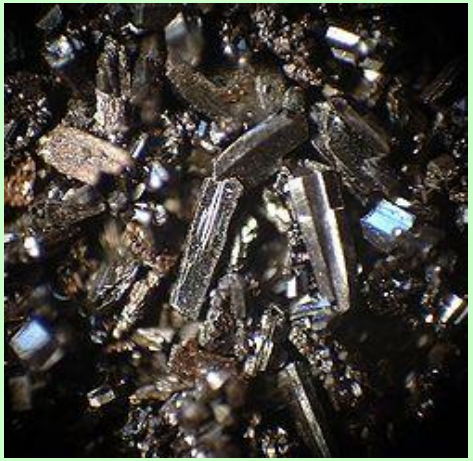

The C60 fullerene in crystalline form

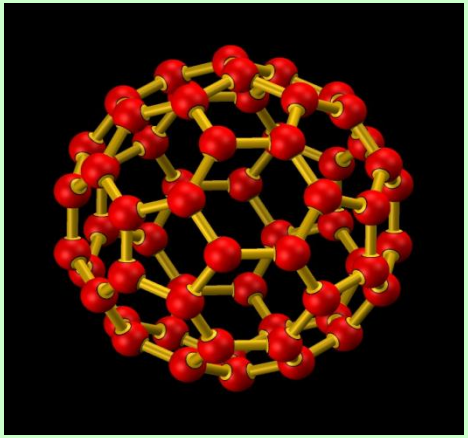

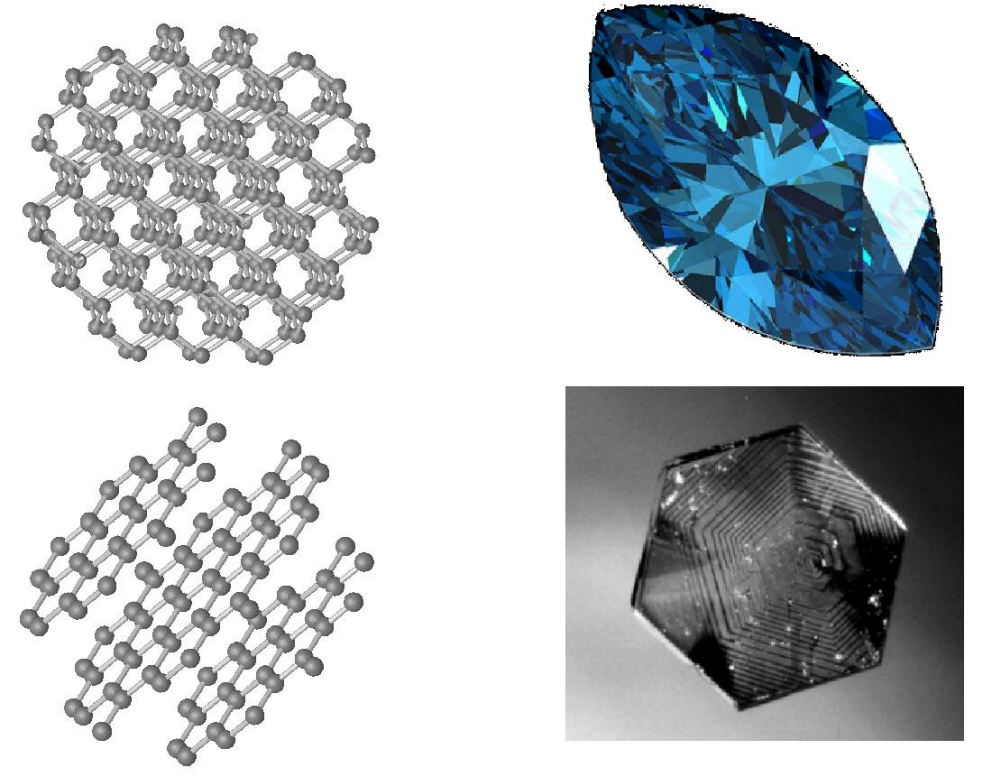

Figure 5.1. Forms of Carbon. Top. Diamond's sp^3 crystalline structure (left) and a crystalline diamond sample (right). Bottom. Graphite's sp^2 crystalline structure (left) and a crystalline graphite sample. (Part of this Figure was reproduced with kind permission of D. Bethune.)

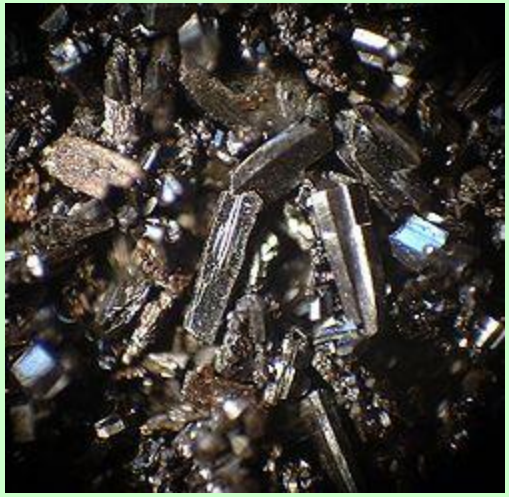

The C60 fullerene in crystalline form

Diamond and Graphite

Le us consider atomic structure of methane (CH_4). There is a serious mis-match between this structure and the modern electronic structure of carbon, $1s^2 2s^2 2p_x^1 2p_y^1$. For a tetrahedrally coordinated carbon (e.g., in methane), the carbon should have 4 orbitals with the correct symmetry to bond to the 4 hydrogen atoms. The modern structure shows that there are only 2 unpaired electrons for hydrogens to share with, instead of the 4 which the simple view requires (Wikipedia, 2010).

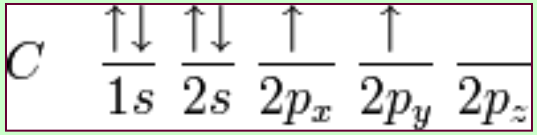

Theory predicts that while exciting a 2*s* electron can move into a 2*p* orbital. The first step in hybridisation is the excitation of one (or more) electrons :

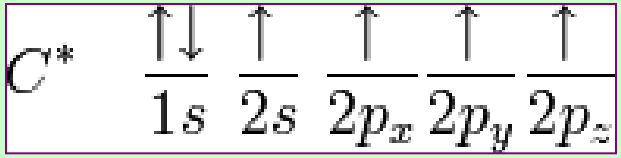

The proton that forms the nucleus of a hydrogen atom attracts one of the lower-energy valence electrons on carbon. This causes an excitation, moving a 2*s* electron into a 2*p* orbital.

sp^3 hybridization

Then, the 2*s* orbital (core orbitals) "mixes" with the three 2*p* orbitals to form four ***sp*³** *hybrids* .

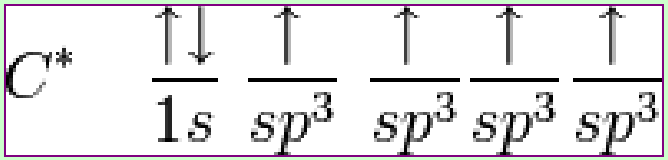

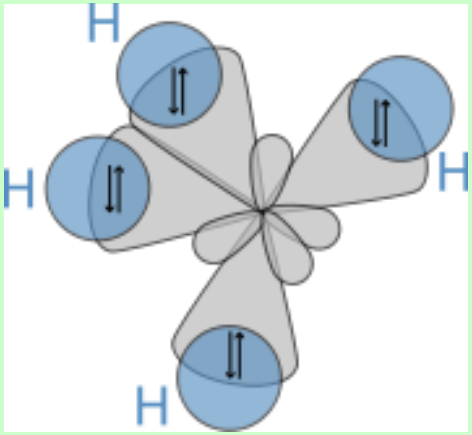

In CH_4, four *sp*3 hybridised orbitals are overlapped by hydrogen's 1*s* orbital, yielding four σ (that is, four single covalent bonds). The four bonds are of the same length and strength (Wikipedia, 2010).

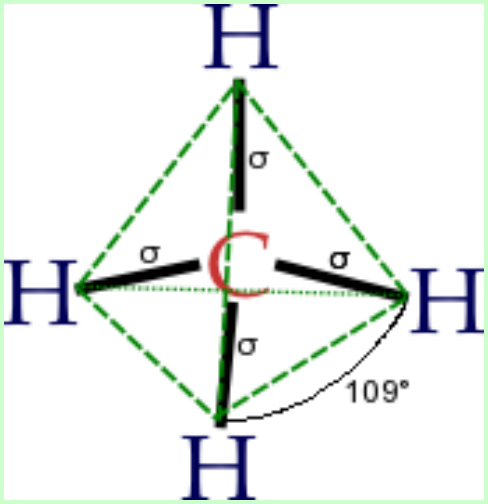

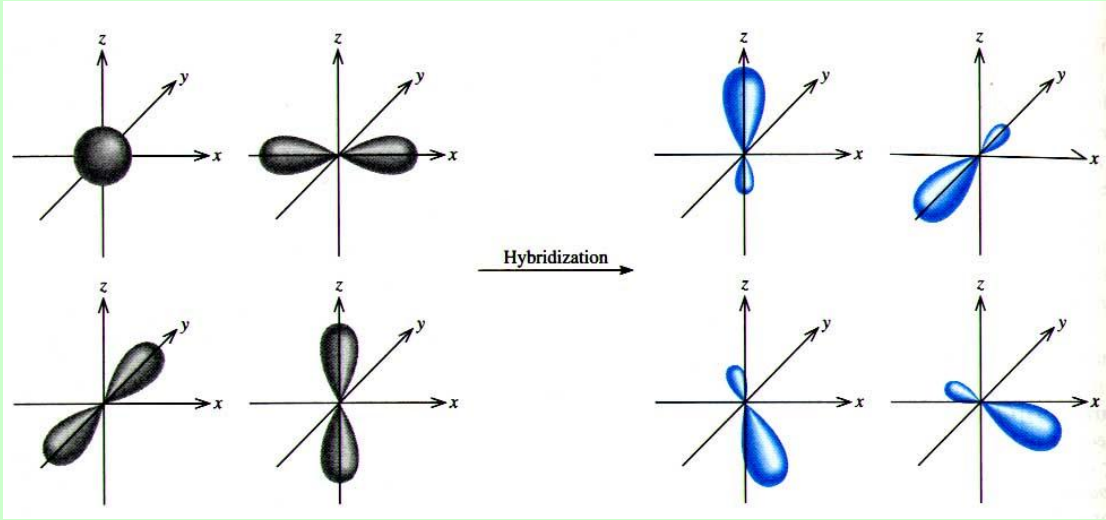

sp^2 hybridization

Ethene (C_2H_4) has a double bond between the carbons. For this molecule, carbon will sp^2 hybridise, because one π bond is required for the double bond between the carbons, and only three *s* bonds are formed per carbon atom. In sp^2 hybridisation the 2_s orbital is mixed with only two of the three available 2*p* orbitals forming a total of 3 *sp*2 orbitals with one p-orbital remaining. :

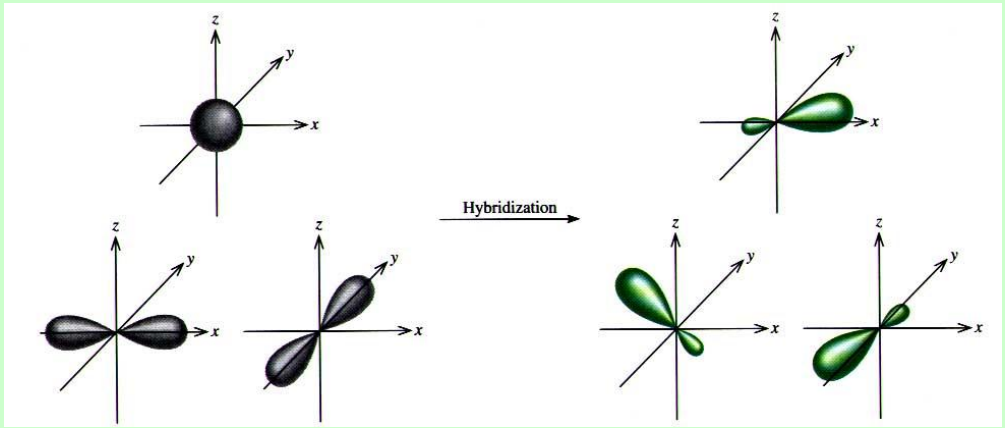

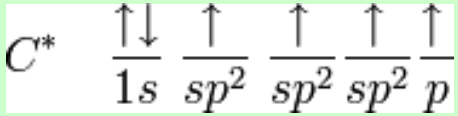

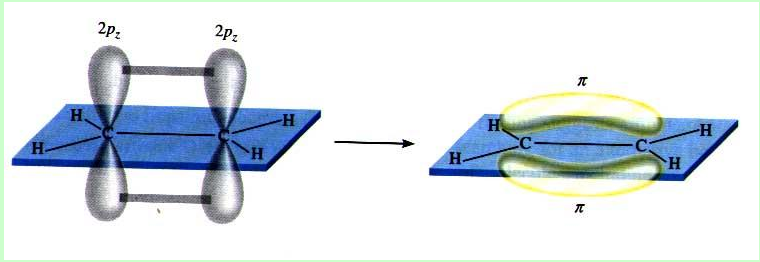

In ethylene the two carbon atoms form a σ bond by overlapping two sp^2 orbitals and each carbon atom forms two covalent bonds with hydrogen by s–sp^2 overlap all with 120° angles. The π bond between the carbon atoms perpendicular to the molecular plane is formed by 2*p*–2*p* overlap. The hydrogen-carbon bonds are all of equal strength and length (Wikipedia, 2010).

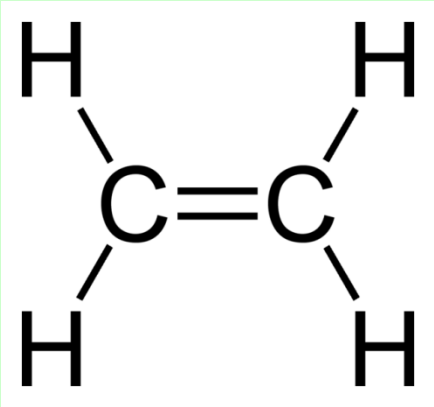

Carbon Bonding: π and σ-bond

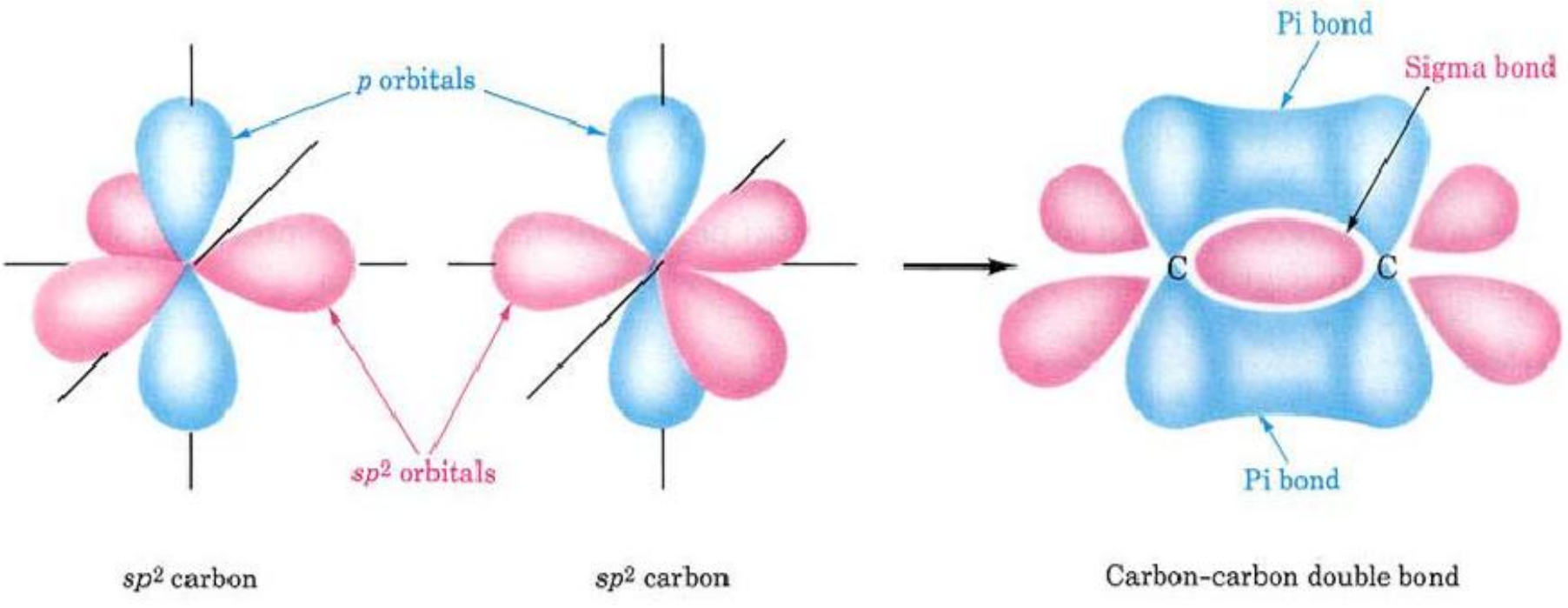

- The electron density of pi bonds is above and below the atoms.
- Delocalized pi bonds provide interesting electrical and optical properties. Fullerenes and nanotubeshave each carbon bonded to three nearest neighbor carbons and thus have pi bonds throughout their structure.

sp hybridization

The chemical bonding in compounds such as acetylene with triple bonds is explained by *sp* hybridization.

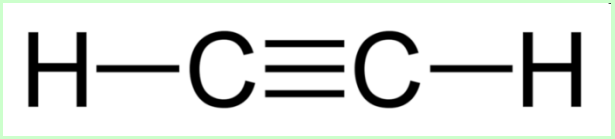

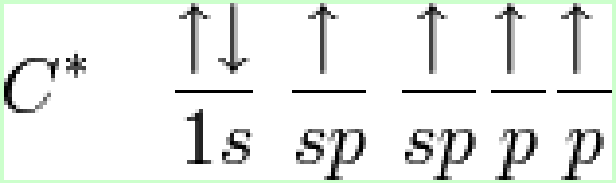

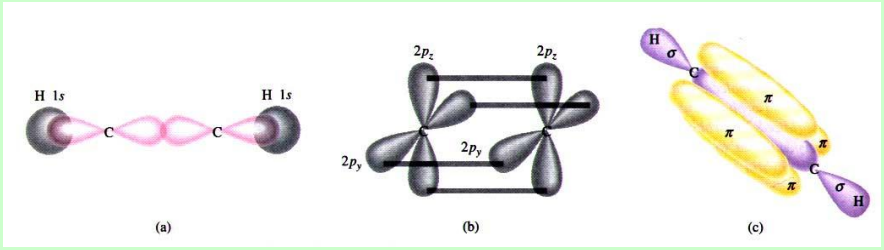

In this model, the 2*s* orbital mixes with only one of the three *p*-orbitals resulting in two *sp* orbitals and two remaining unchanged *p* orbitals. The chemical bonding in acetylene (C_2H_2) consists of *sp*–*sp* overlap between the two carbon atoms forming a σ bond and two additional π bonds formed by *p*–*p* overlap. Each carbon also bonds to hydrogen in a sigma *s*–*sp* overlap at 180° angles (Wikipedia,2010).

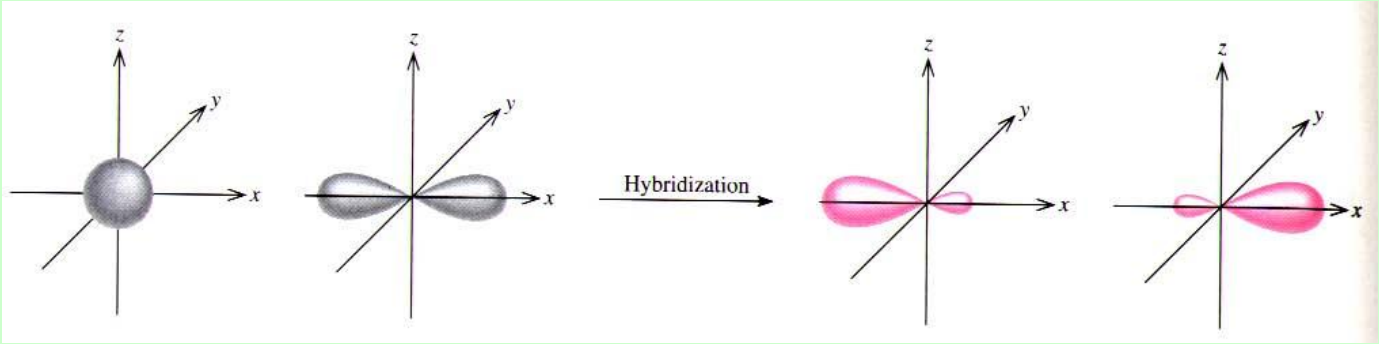

Diamond, Graphite, Fullerene, Nanotube, Graphene

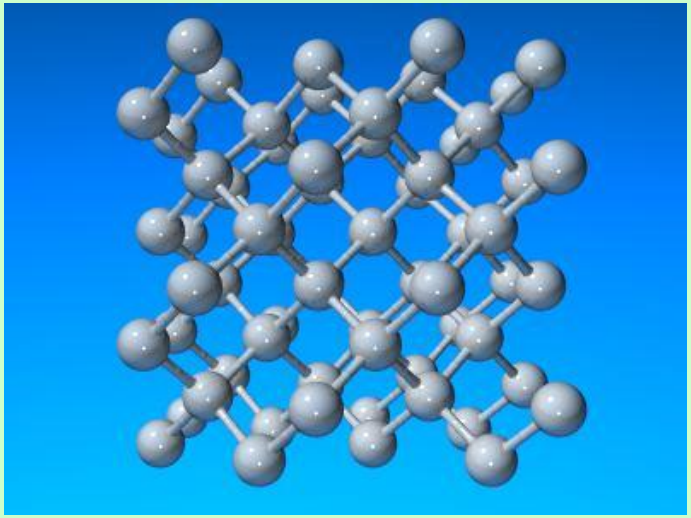

Diamond (sp^3 bonding)

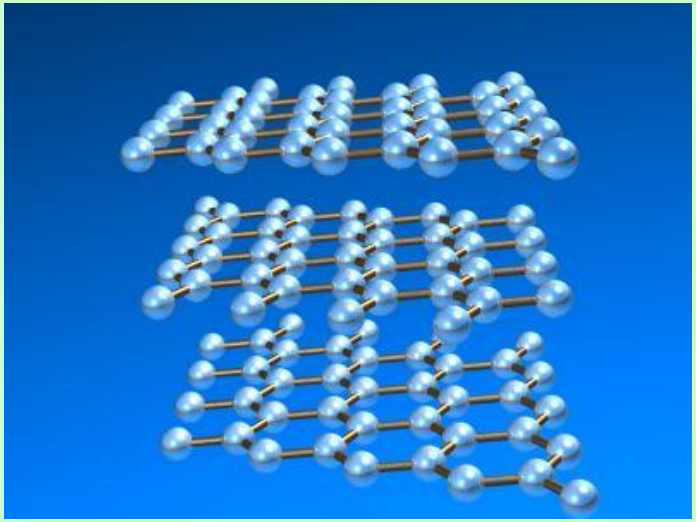

Graphite, Graphene sp^2bonding)

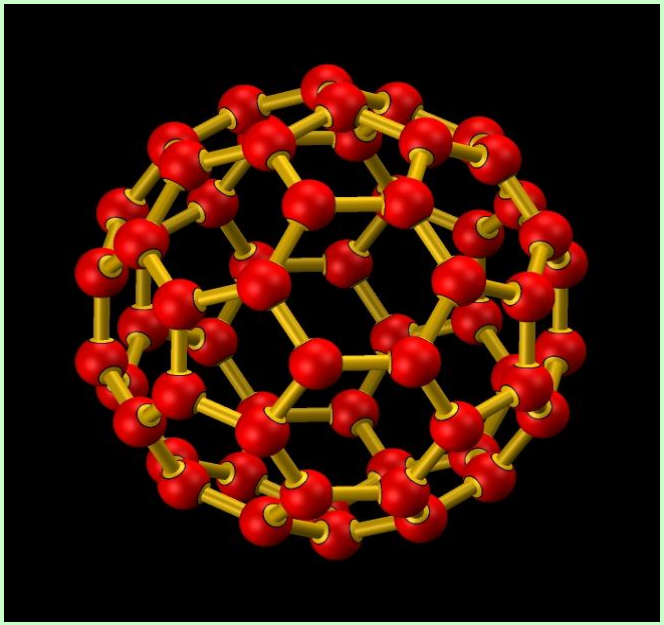

Fullerene

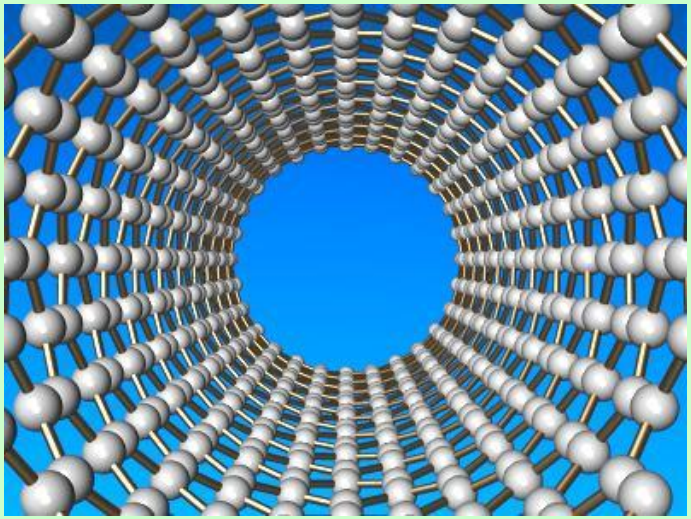

Nanotube

Diamond, Graphite, Fullerene, Nanotube, Graphene

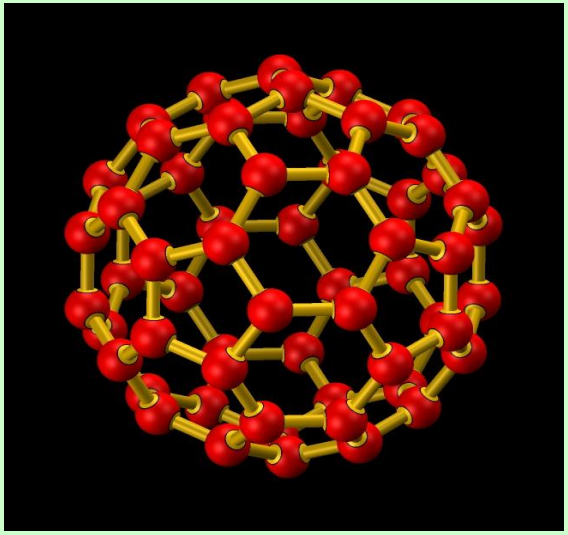

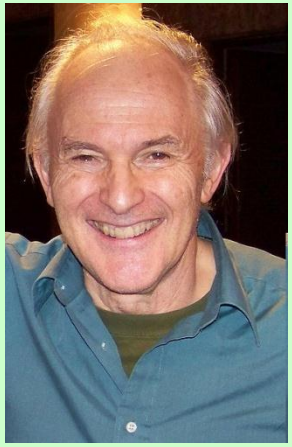

Harold Kroto

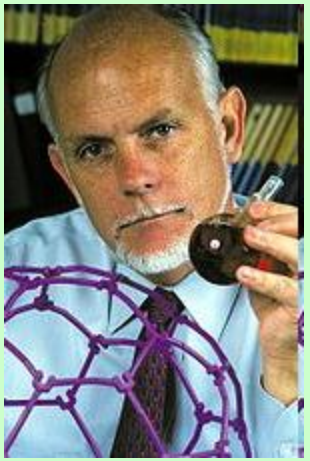

Richard Smalley

1985: British chemist Harry Kroto studied molecules with exactly sixty carbon atoms found near red giant stars. Kroto collaborated with Richard Smalley and Robert Curl to recreate the conditions in the Smalley's laboratory and form C60 molecules by laser vaporization of graphite.

The scientists hypothesized that the molecules were made of hexagonal carbon rings blasted apart from the graphite structure, and that the molecule must be spheroid to satisfy valence requirements Buckyball which generated so much excitement among scientists and won Curl, Kroto, and Smalley the 1996 Nobel prize in chemistry.

Five years later, Kratschmer and Huffman discovered a simple method of making these molecules and a new branch of Chemistry was born. The method consists of sending a beam current between two nearby graphite electrodes in an inert atmosphere. The resulting carbon plasmas are between the electrodes cool into sooty residue from which many fullerenes can be isolated.

Nanotubes

A 2006 editorial written by Marc Monthioux and Vladimir Kuznetsov in the journal *Carbon* described the interesting and often misstated origin of the carbon nanotube. A large percentage of academic and popular literature attributes the discovery of hollow, nanometer-size tubes composed of graphitic carbon to Sumio Iijima of NEC in 1991

In 1952 L. V. Radushkevich and V. M. Lukyanovich published clear images of 50 nanometer diameter tubes made of carbon in the Soviet Journal of Physical Chemistry. This discovery was largely unnoticed, as the article was published in the Russian language, and Western scientists' access to Soviet press was limited during the Cold War. It is likely that carbon nanotubes were produced before this date, but the invention of the transmission electron microscope (TEM) allowed direct visualization of these structures (Wikipedia).

Carbon nanotubes have been produced and observed under a variety of conditions prior to 1991. A paper by Oberlin, Endo, and Koyama published in 1976 clearly showed hollow carbon fibers with nanometer-scale diameters using a vapor-growth technique. Later, Endo has referred to this image as a single-walled nanotube

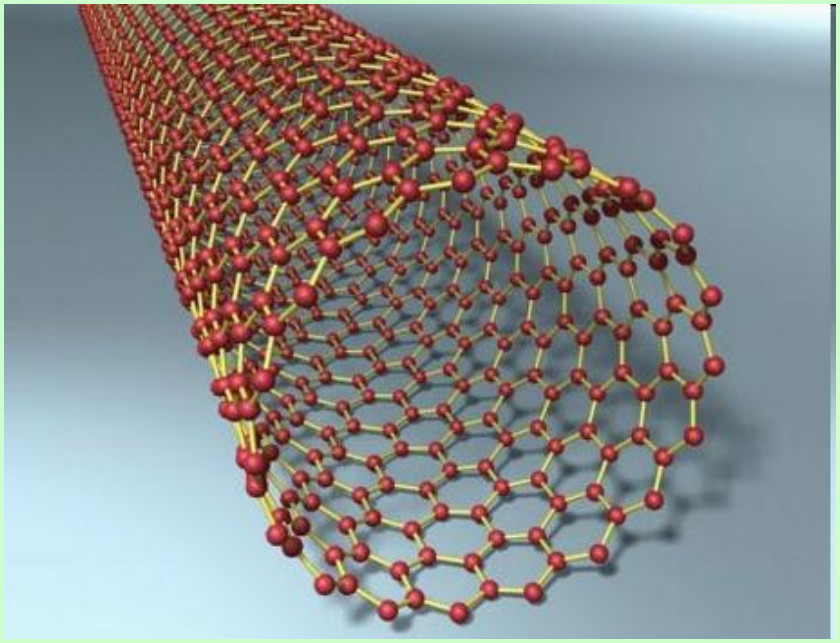

In 1979 John Abrahamson presented evidence of carbon nanotubes at the 14th Biennial Conference of Carbon at Pennsylvania State University. The conference paper described carbon nanotubes as carbon fibers which were produced on carbon anodes during arc discharge. A characterization of these fibers was given as well as hypotheses for their growth in a nitrogen atmosphere at low pressures (Wikipedia, 2010).

Graphene

Graphene is a one-atom-thick planar sheet of sp^2bonded carbon atoms that are densely packed in a honeycomb crystal lattice. The term Graphene was coined as a combination of graphite and the suffix – ene by Hans-Peter Boehm, who described single-layer carbon foils in 1962.

The carbon-carbon bond length in graphene is about 0.142 nm. Graphene sheets stack to form graphite with an interplanar spacing of 0.335 nm, which means that a stack of 3 million sheets would be only one millimeter thick. Graphene is the basic structural element of some carbon allotropes including graphite, charcoal, carbon nanotubes, and fullerenes. The Nobel Prize in Physics for 2010 was awarded to Andre Geim and Konstantin Novoselov "for groundbreaking experiments regarding the two-dimensional material graphene“ Wikipedia, 2010).

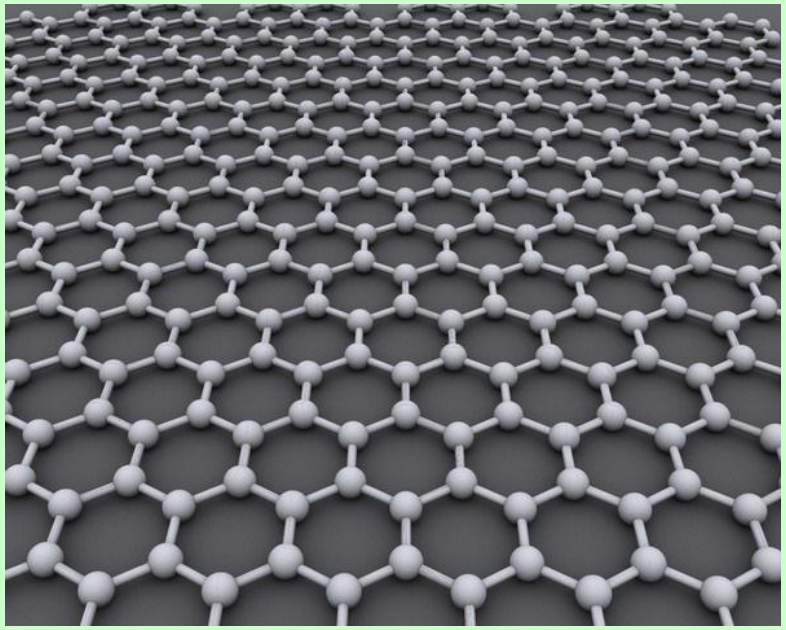

Andre Geim, left, and Dr Konstantin Novoselov

Raman Spectroscopy of the Graphite

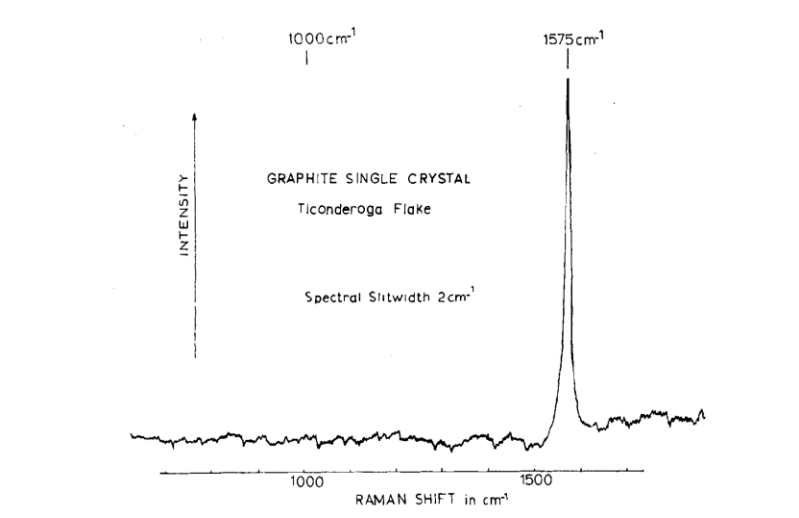

Raman spectrum of single crystal of graphite (From Tuinstra, Koenig, *J. Chem. Phys*. **55** 1125, 1970).

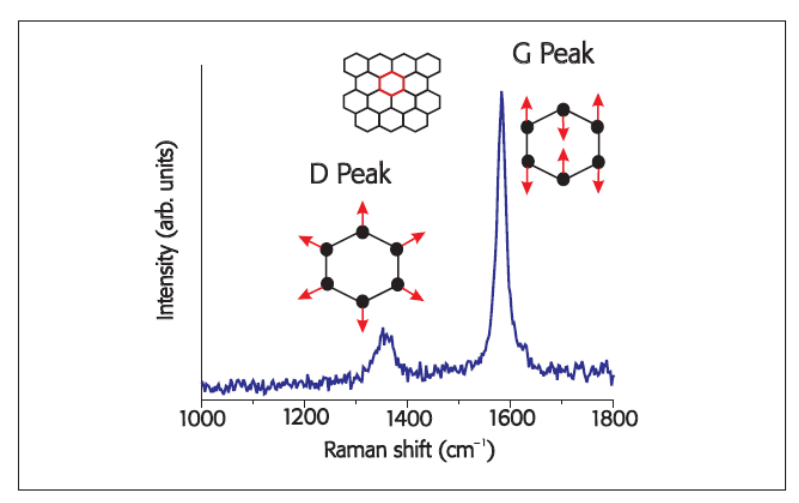

Raman spectrum (514 nm) of highly orientated pyrolitic graphite (J. Filik, *Spectrosc. Europe*, 2005)

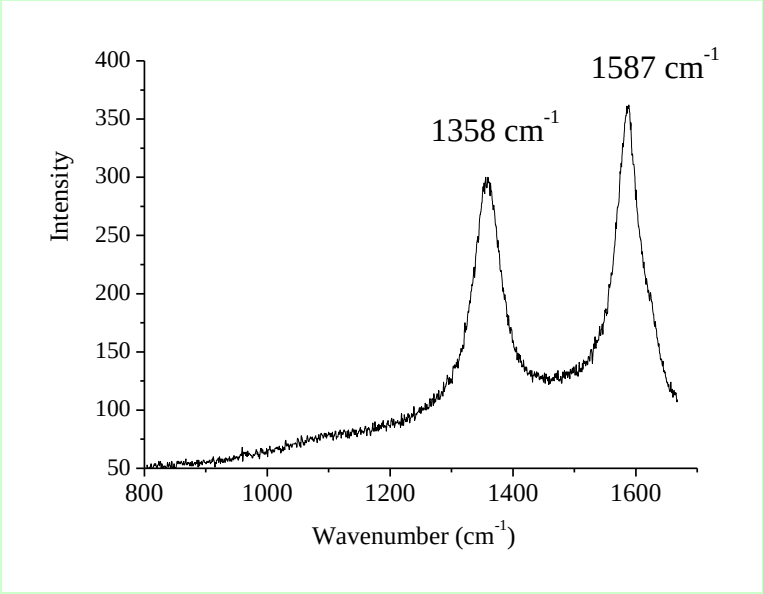

Raman spectrum of turbostratic graphite.

The 1571 cm $^{-1}$ peak (called the "G" peak, after crystalline graphite) is the only Raman active mode of the infinite lattice. The other peak (the "D" peak from disordered graphite) is caused by breakdown of the solid-state Raman selection rules.

Raman spectroscopy of the graphite

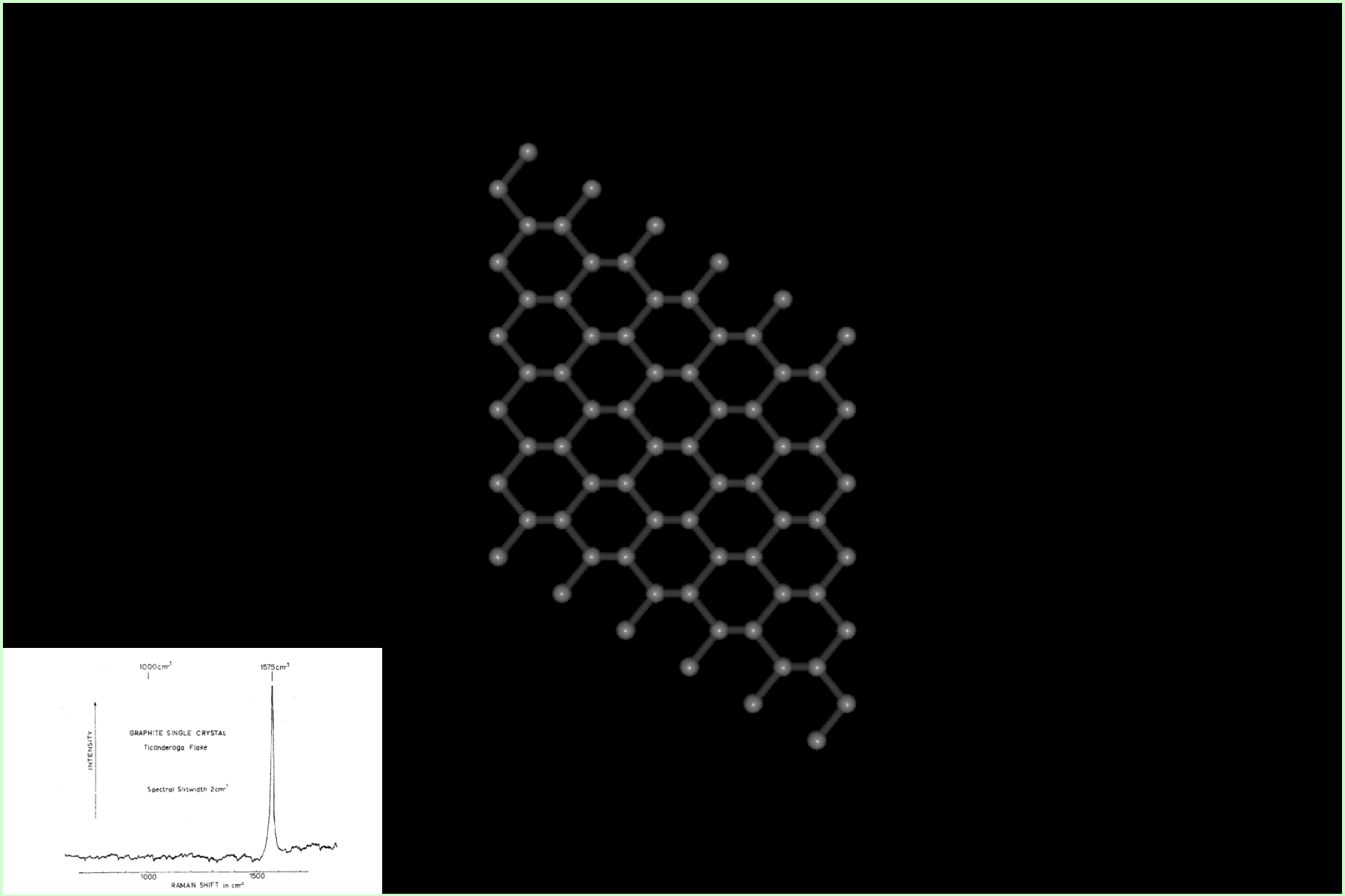

Raman Spectrum of Diamond

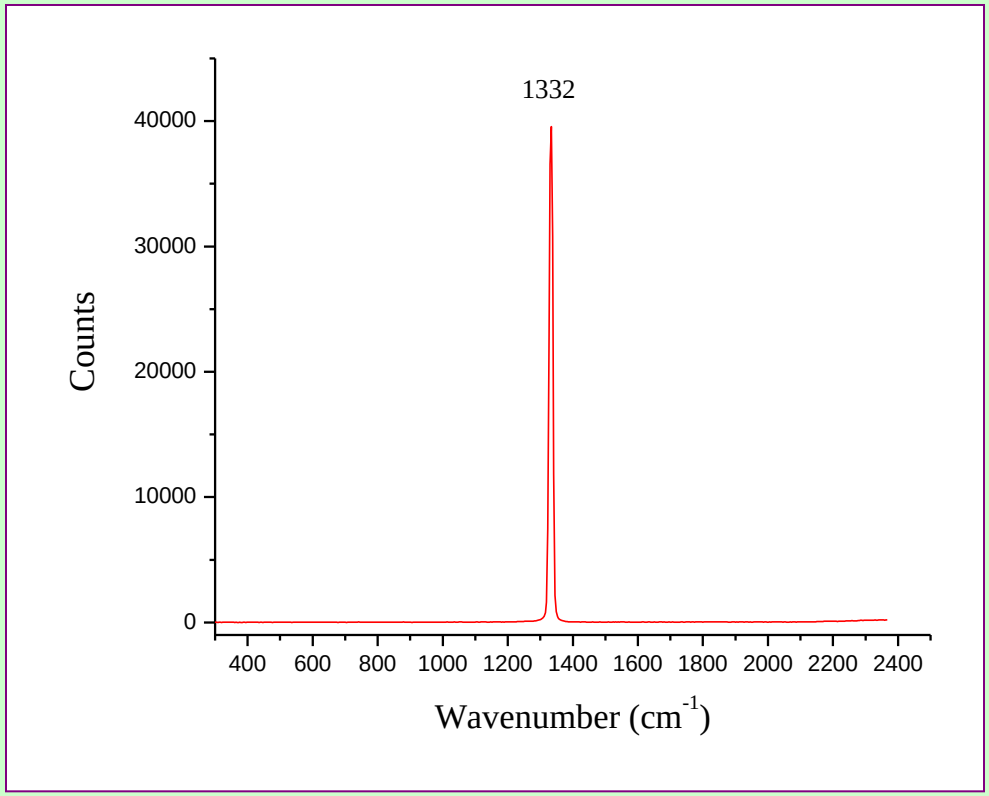

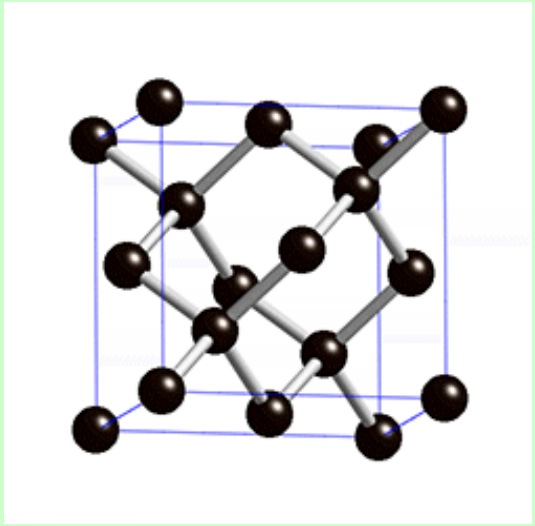

Raman spectrum (224 nm) of diamond

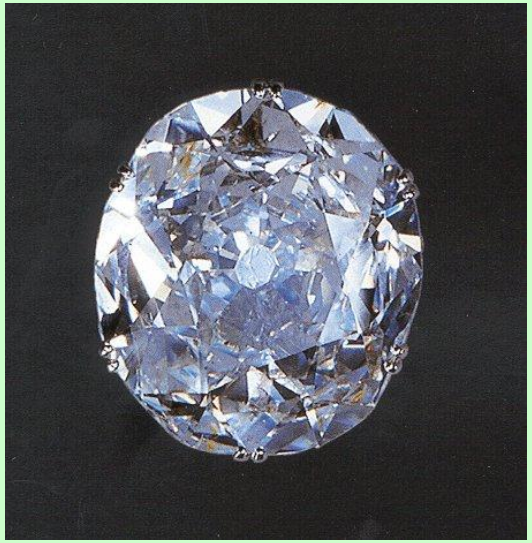

Laser Heating in DAC of graphite, 50 GPa, 1500 K)

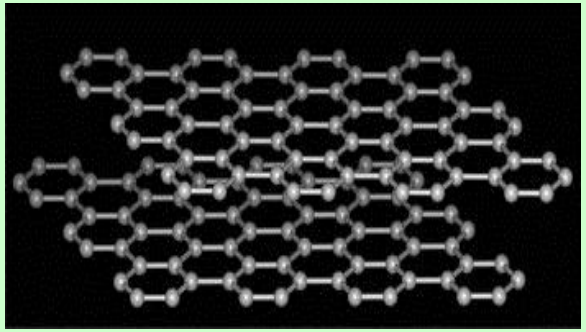

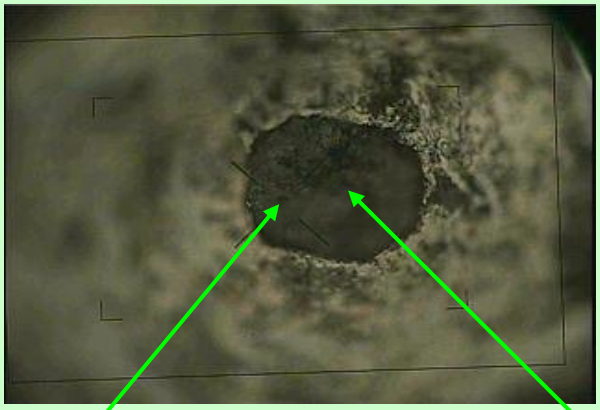

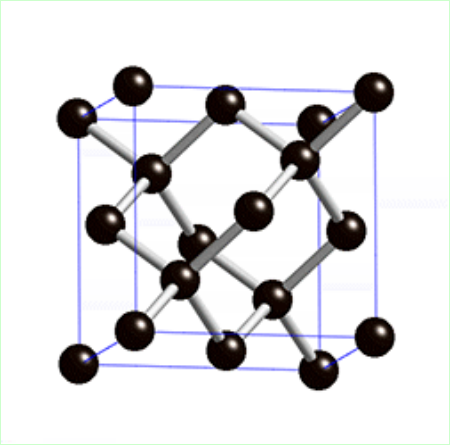

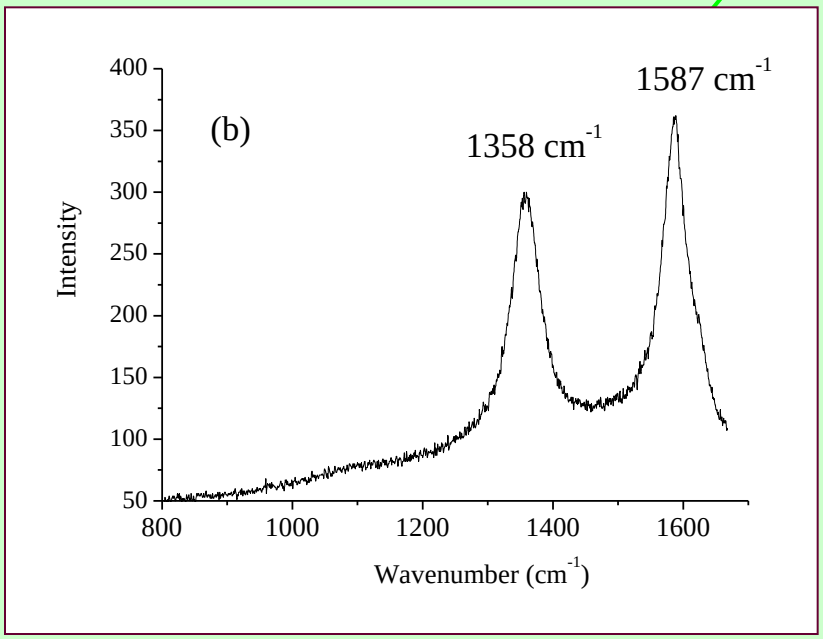

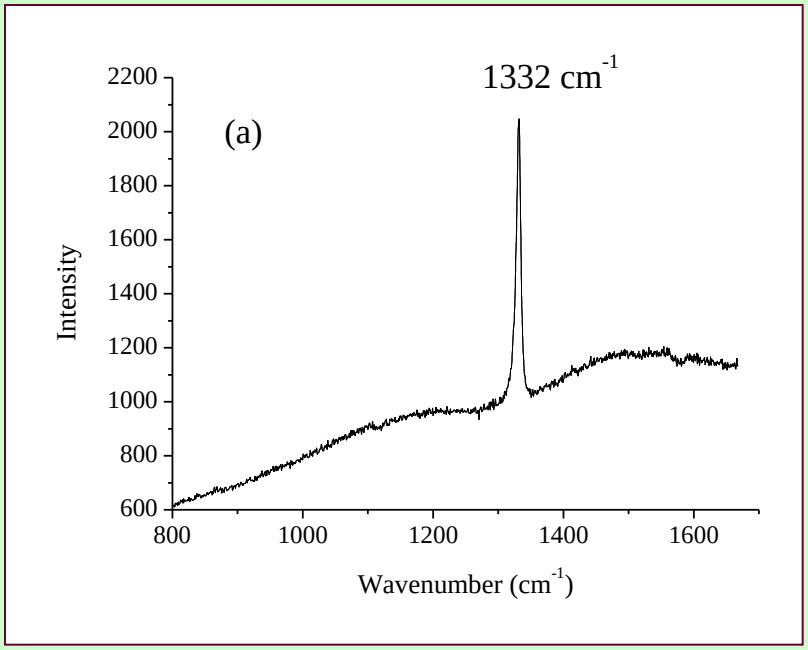

Graphite after laser heating at 50 GPa and 1500 K

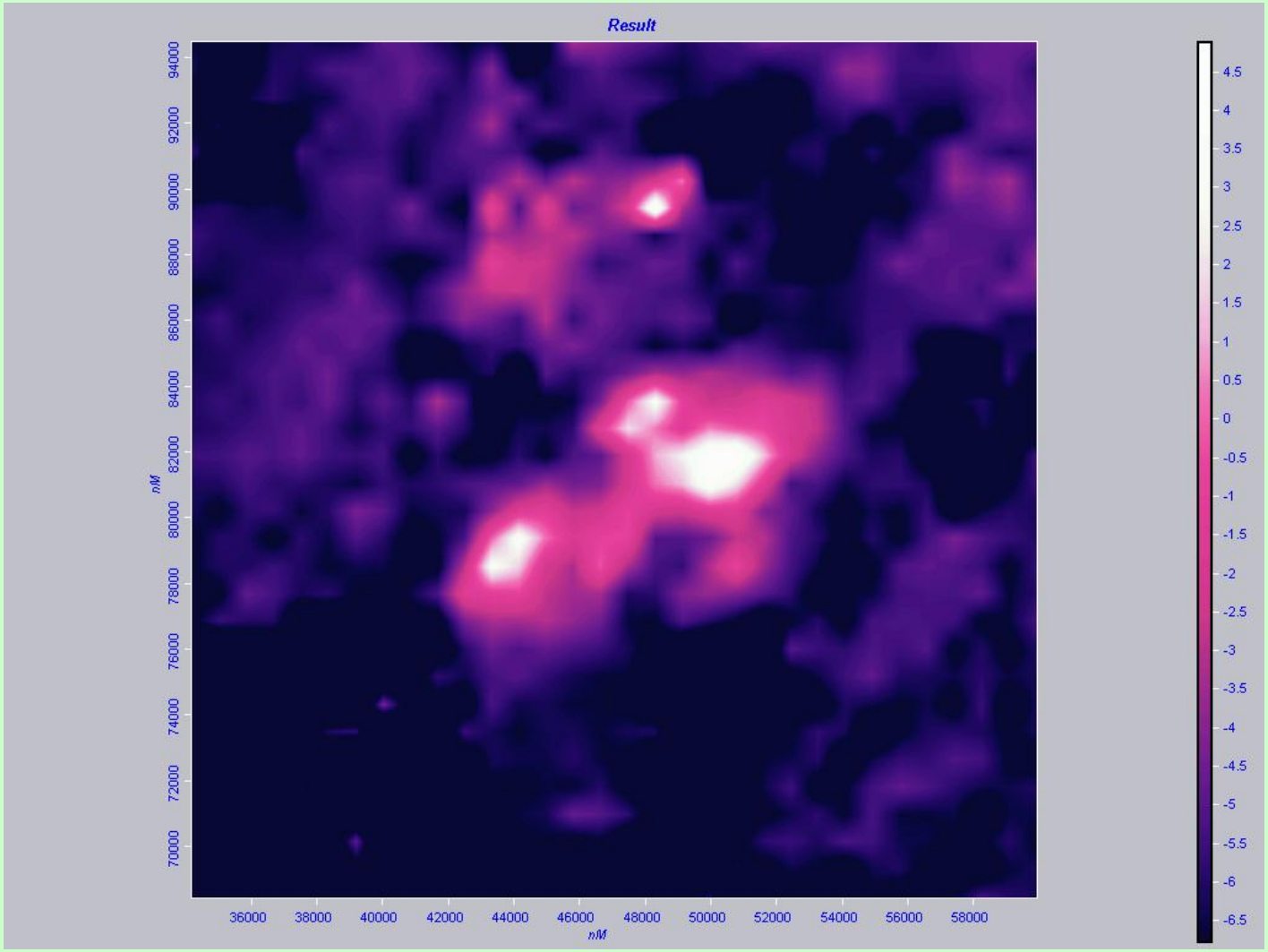

Intensity XY mapping (16 x 16 μm) of peak 1332 cm^{-1}

Raman spectroscopy of C_{60}

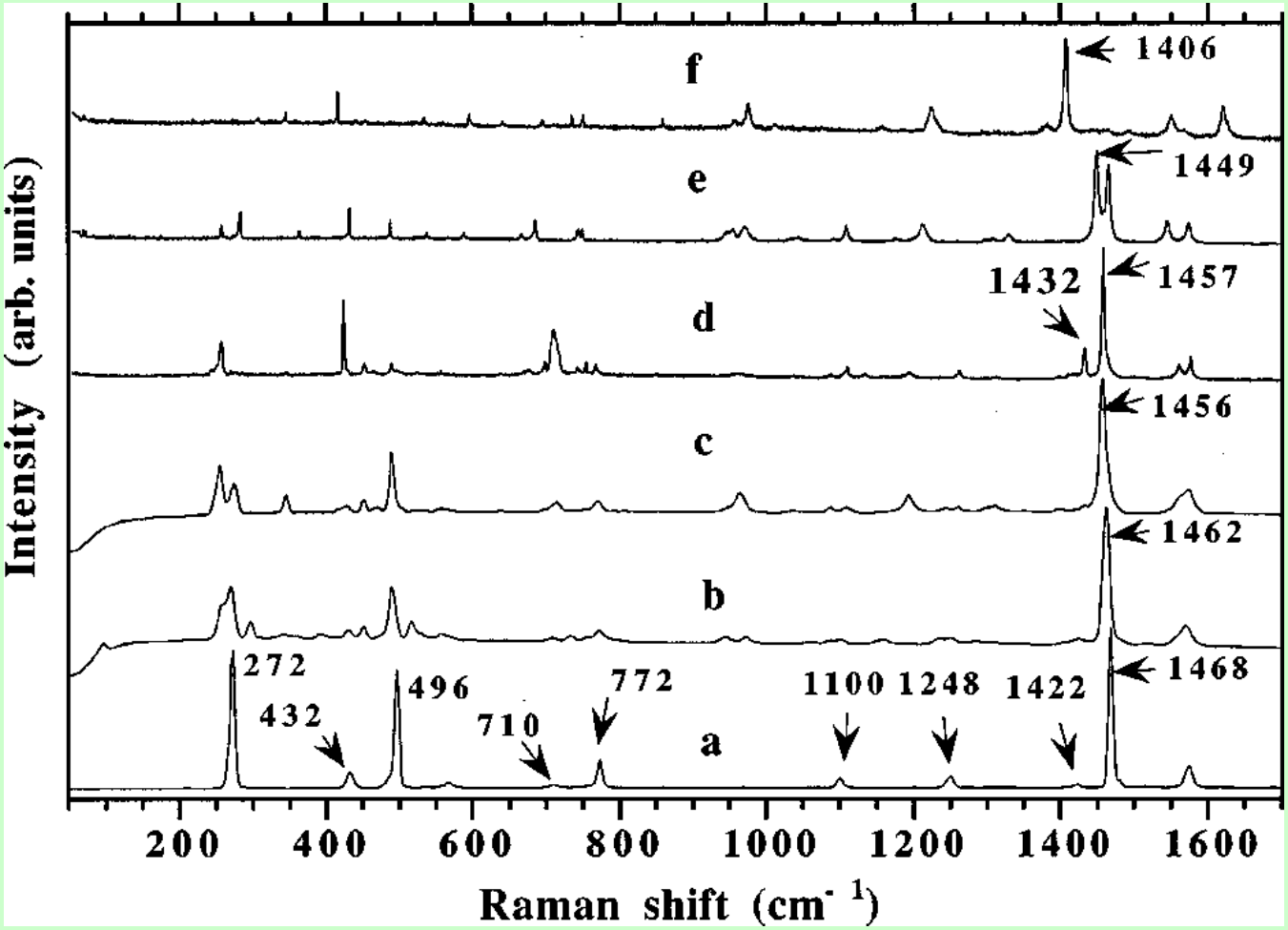

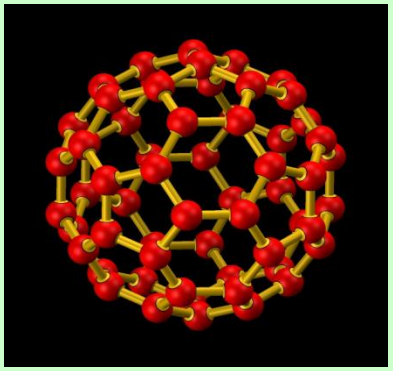

The isolated C60 molecule possesses *Ih* symmetry, its 174 vibrations being distributed between 46 distinct modes according to irreducible representation. From these, because of selection rules, only four modes of F_{1u} symmetry are IR active and ten modes of A_g and H_g symmetry are allowed in Raman spectra; the remaining 32 modes are silent

Raman spectra of the pristine C60 (a), dimerized state (b) , and orthorombic (O) phase (c), excited by a 1064-nm line; those of the *O (*d), tetragonal (e), and rhombohedral (f) phases, excited by a 568.2-nm line (Davidov, et al., *PRB* 2000)

Raman Spectroscopy of Nanotubes

Raman spectrum of single-wall carbon nanotubes (Wikipedia, 2010)

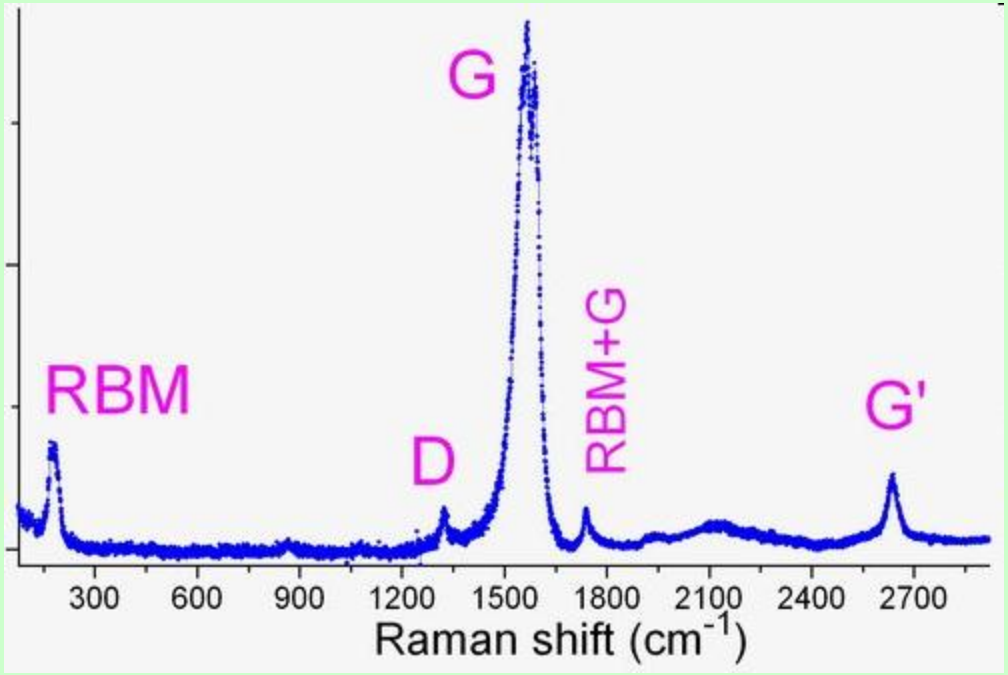

G' mode is actually the second overtone of the defect-induced D mode (and thus should logically be named D'). Its intensity is stronger than that of the D mode due to different selection rules. In particular, D mode is forbidden in the ideal nanotube and requires a structural defect, providing a phonon of certain angular momentum, to be induced. In contrast, G' mode involves a "self-annihilating" pair of phonons and thus does not require defects. The spectral position of G' mode depends on diameter, so it can be used roughly to estimate the SWCNT diameter.

Other overtones, such as a combination of RBM+G mode at ~1750 cm^{-1}, are frequently seen in CNT Raman spectra. However, they are less important and are not considered here.

Radial breathing mode (RBM) corresponds to radial expansion-contraction of the nanotube. Therefore, its frequency f_{RBM} (in cm^{-1}) depends on the nanotube diameter d (in nanometers) and can be estimated as $f_{RBM} = 223/d + 10$, which is very useful in deducing the CNT diameter from the RBM position. Typical RBM range is 100–350 cm^{-1} (Wikipedia, 2010).

Another very important mode is the G mode (G from graphite). G band in SWCNT is shifted to lower frequencies relative to graphite (1580 cm^{-1}) and is split into several peaks. The splitting pattern and intensity depend on the tube structure and excitation energy; they can be used, though with much lower accuracy compared to RBM mode, to estimate the tube diameter and whether the tube is metallic or semiconducting.

D mode is present in all graphite-like carbons and originates from structural defects. Therefore, the ratio of the G/D modes is conventionally used to quantify the structural quality of carbon nanotubes. High-quality nanotubes have this ratio significantly higher than 100.

Raman Spectroscopy of Nanotubes

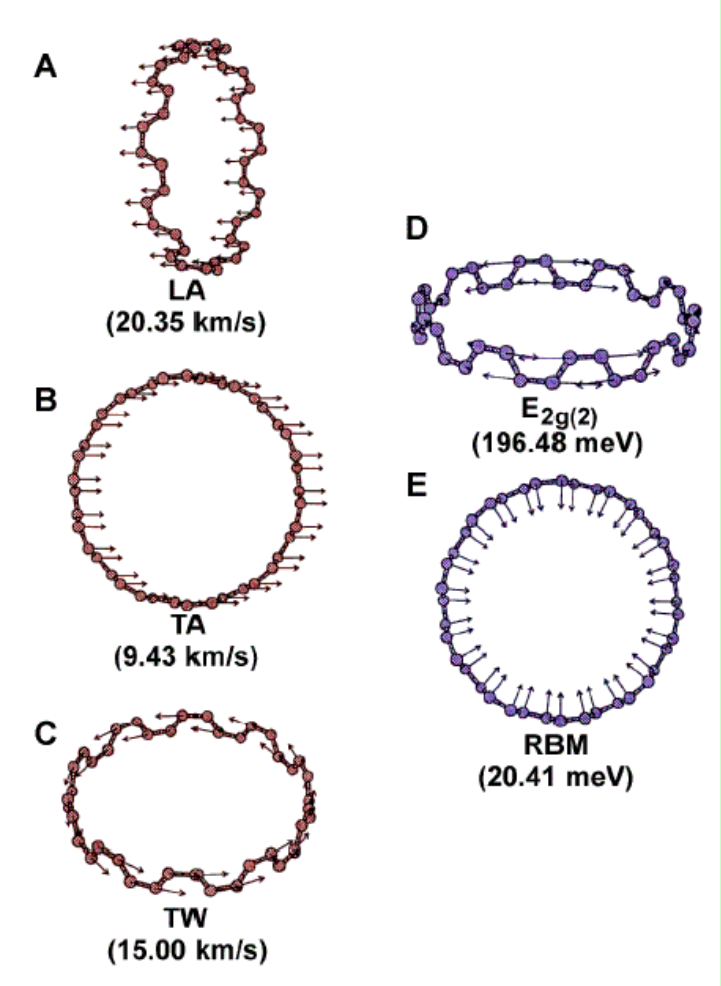

Important vibrational modes in SWNTs, illustrated for a (10,10) SWNT. (a) Longitudinal acoustic mode. (b) Transverse acoustic mode (doubly degenerate). (c) Twisting (acoustic) mode. (d) $E_{2g(2)}$ mode (doubly degenerate). (e) A_{1g} mode (radial breathing mode). Calculated sound velocities are indicated for the acoustic modes, (a-c). (d-e) are Raman active optical modes. (From Benes Z)

Radial breathing mode (RBM) corresponds to radial expansion-contraction of the nanotube. Therefore, its frequency f_{RBM} (in cm^{-1}) depends on the nanotube diameter d (in nanometers) and can be estimated as $f_{\mathrm{RBM}} = 223/\mathrm{d} + 10$, which is very useful in deducing the CNT diameter from the RBM position. Typical RBM range is 100–350 cm^{-1} (Wikipedia, 2010).

Raman active modes of g-BC_3

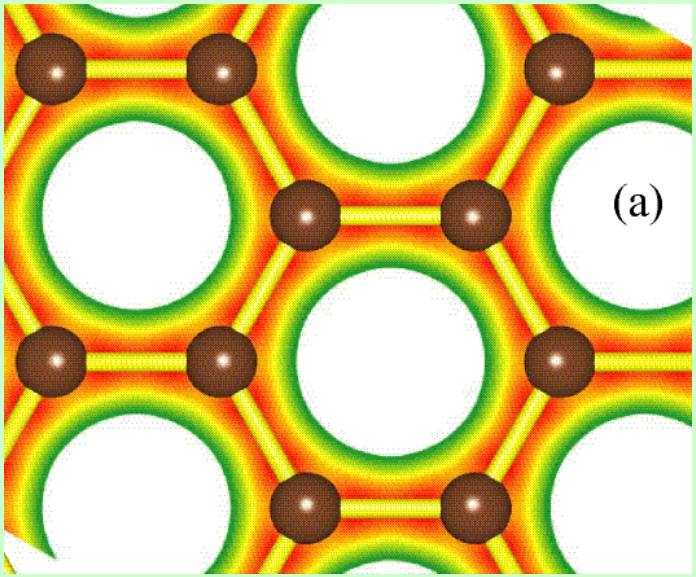

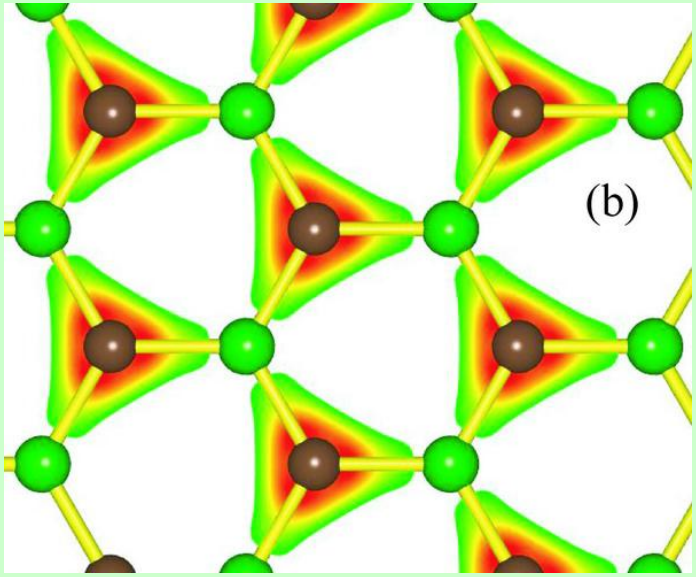

Electronic charge distribution (a) in graphene sheet, (b) in graphitic BC, and (c) in graphitic BC3.

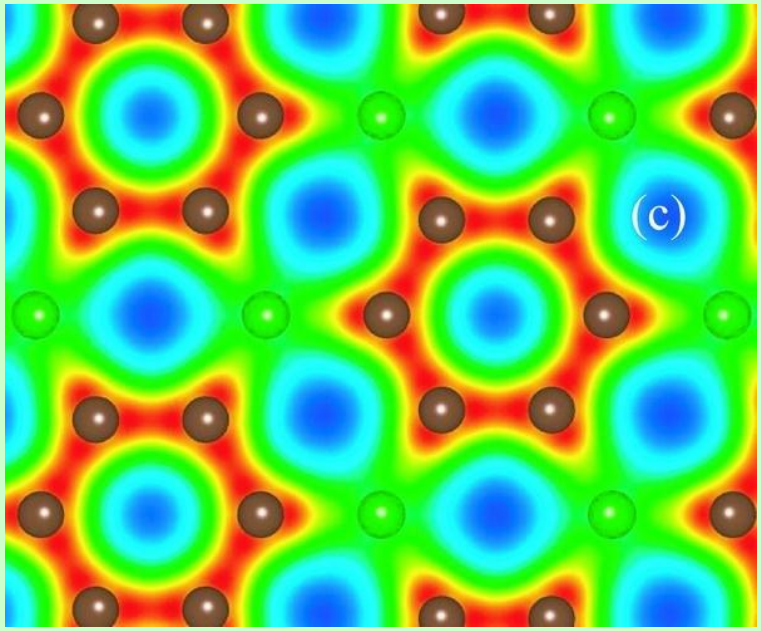

Images of the electronic structures were simulated by Prof. *Ted Lowther*, University of the Witwatersrand, Johannesburg, South Africa

Visible (514 nm) Raman spectra of the *g*-BC_5

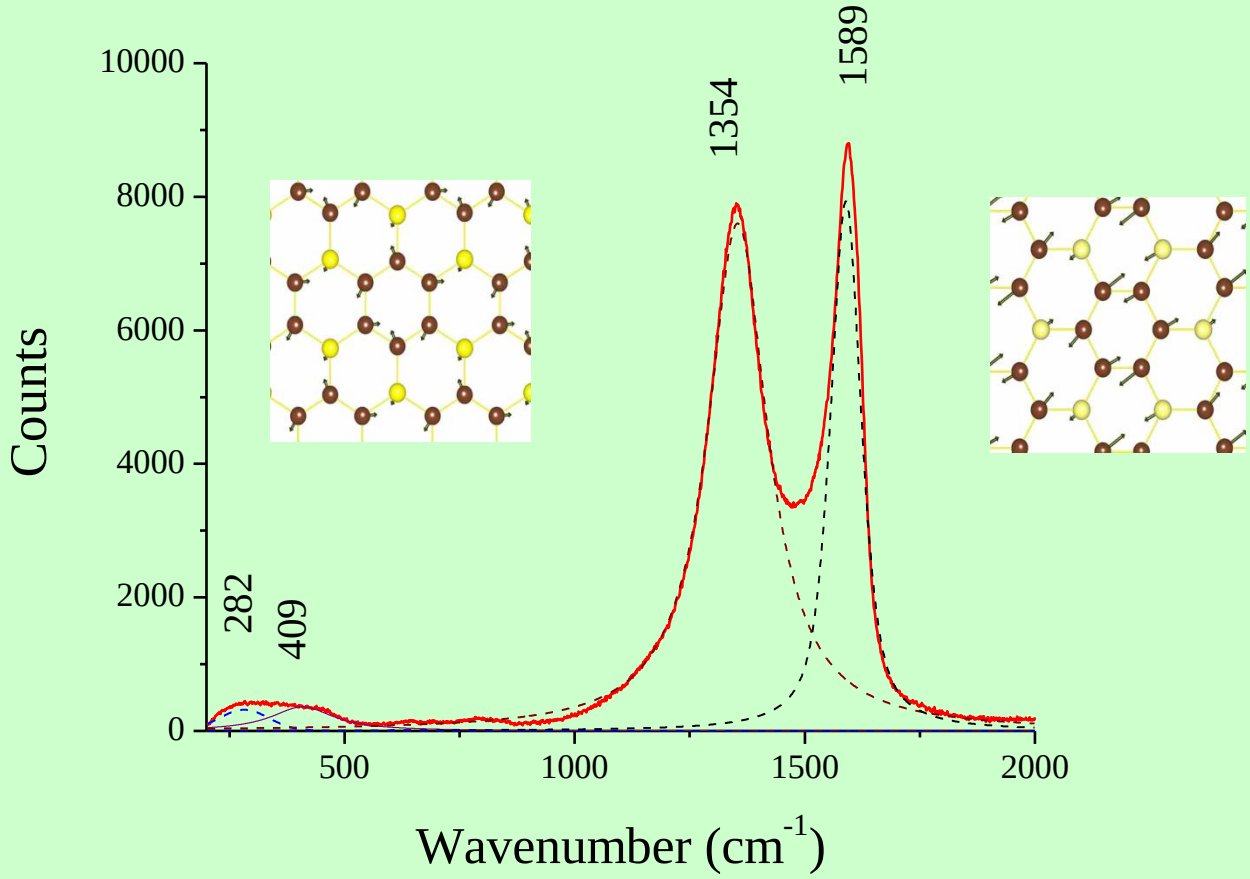

Visible Raman spectrum taken with ×20 objective; integration time was 1 min.; laser power on sample was 2 mW (Zinin *et al*. Diamond Related Mater. 2009).

Raman active modes of g-BC_3

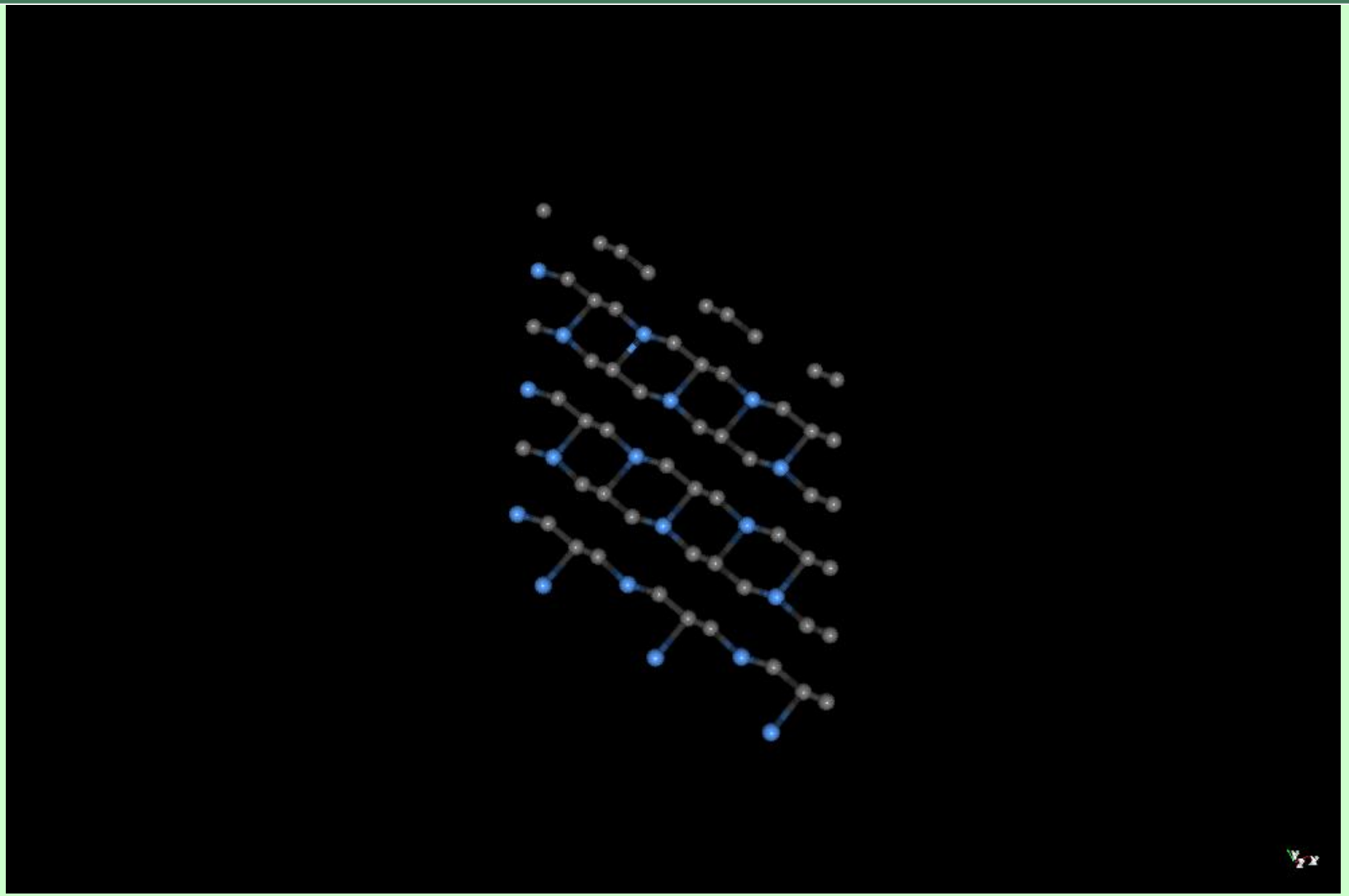

High energy vibration of g-BC_3 calculated at 1550 cm^{-1}. Atomic displacements are slightly away from the interatomic bond unlike graphene

(Simulations by Prof. *Ted Lowther*, University of the Witwatersrand, Johannesburg, South Africa).

Raman active modes of *g*-BC_3

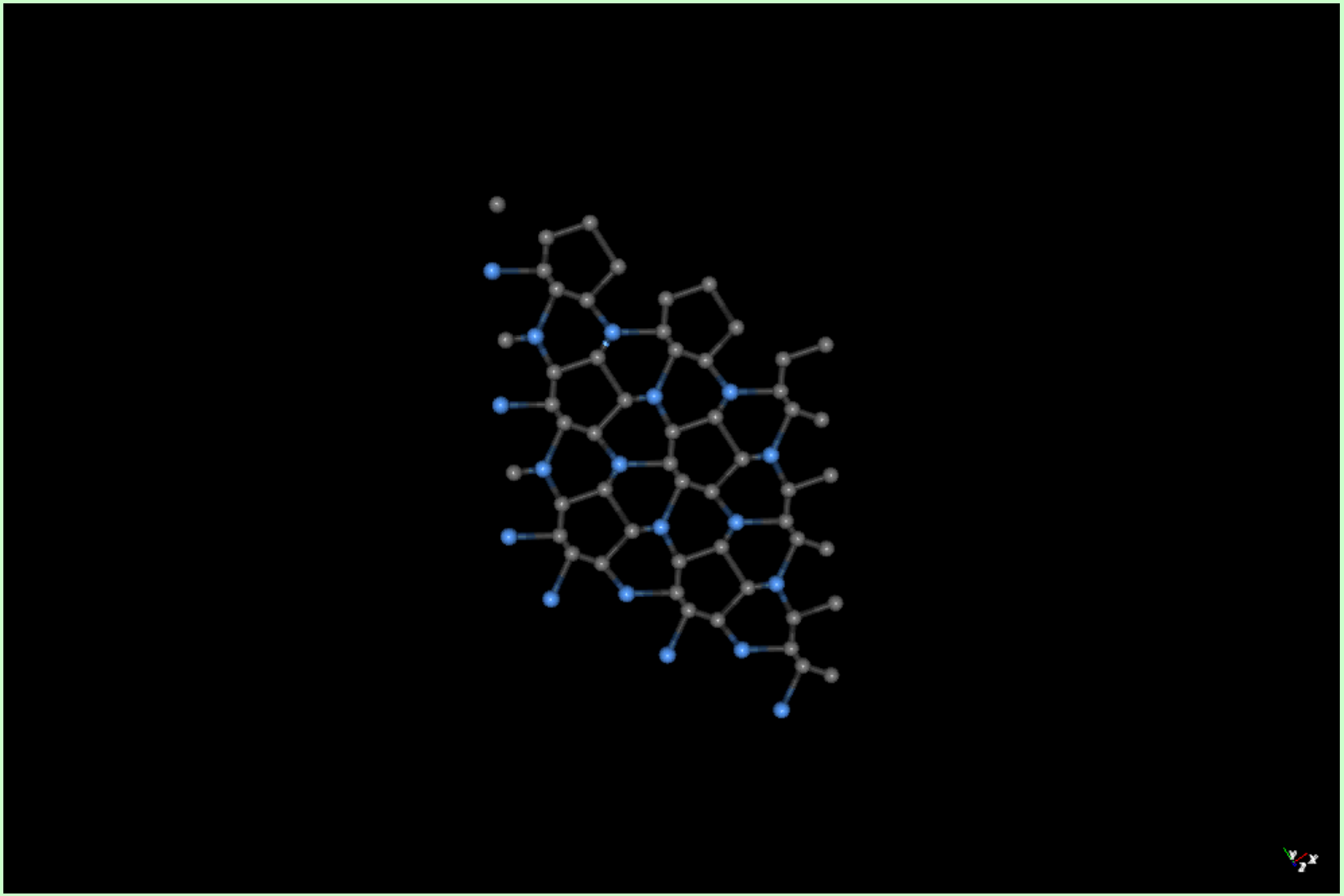

Second highest energy vibration of the *g*-BC_3 vibration structure calculated at 1347 cm^{-1} (Lowther *et al*., *PRB*, 2009)..

The UV (244 nm) and visible (514 nm) Raman spectra of the *g*-BC_4(I)

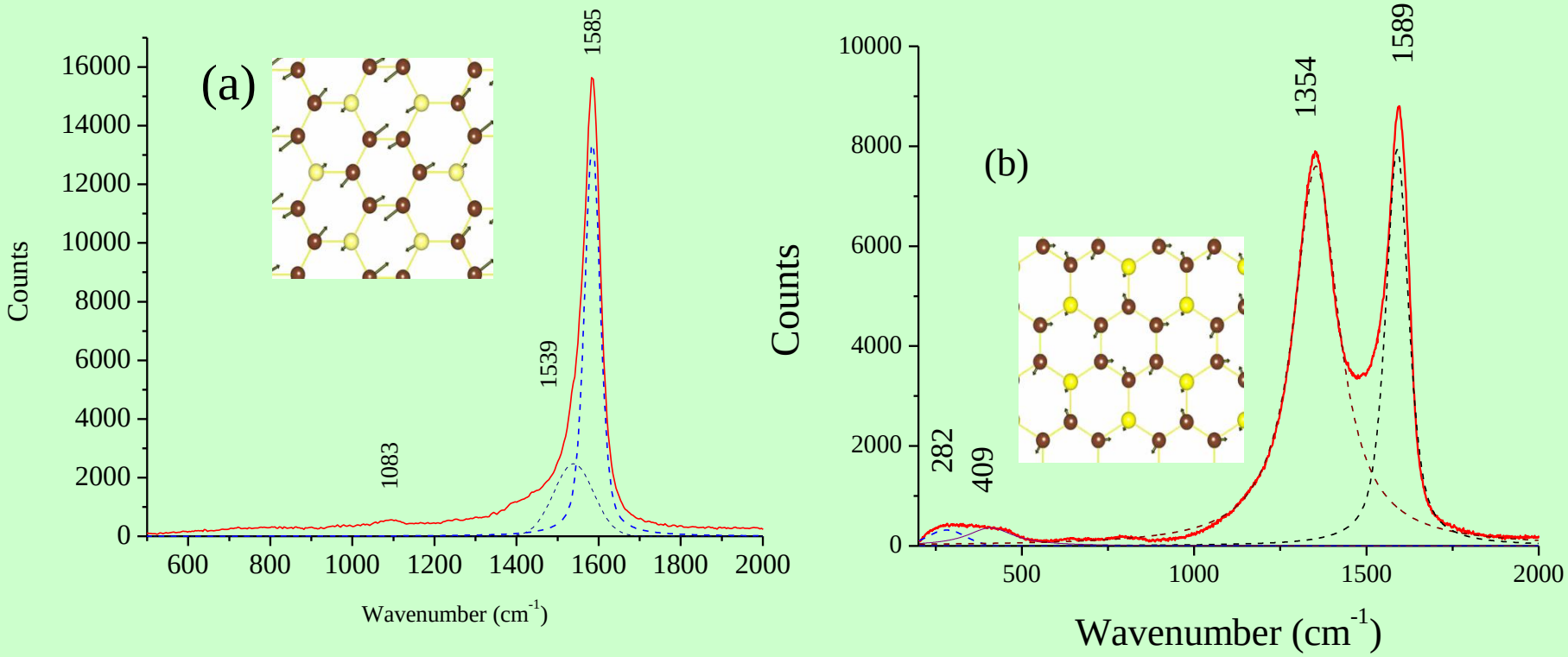

(a) the UV Raman spectrum taken with UV×40 objective; integration time was 10 min; laser power on sample was 0.05 mW; (b) visible Raman spectrum taken with ×20 objective; integration time was 1 min.; laser power on sample was 2 mW (Zinin *et al*. Diamond Related Mater. 2009).

Structure of *g*-C_3N_4 phases

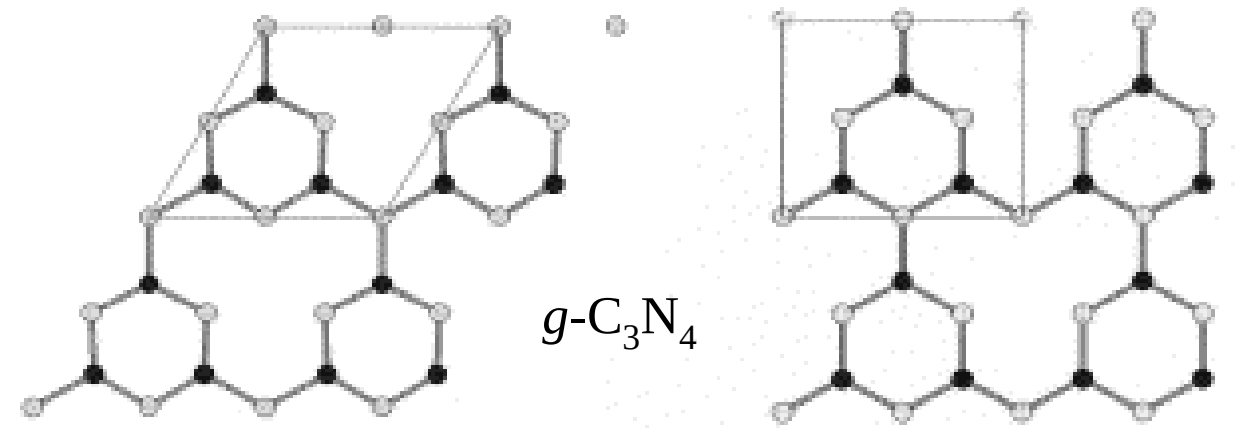

Alves, *Solid State Comm*. **109**, 697 (1999).

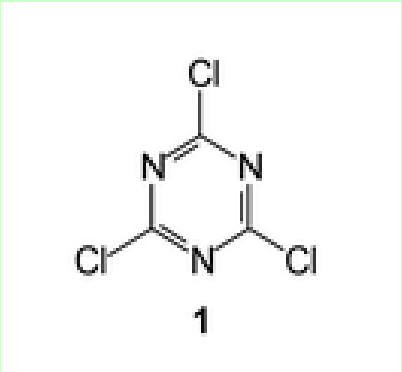

Cyanuric chloride

Benzene-thermal reaction between $C_3N_3Cl_3$ and $NaNH_2$ (nitriding solvent) at 200 C for 8–12 h.

$$C_3N_3Cl_3+3NaNH_2 \rightarrow \quad g\text{-}C_3N_4+3NaCl+2NH_3$$

Guo et al. *Chem. Phys. Lett*. **380** 84 (2003).

9:04 AM

Raman spectroscopy of the g-C_3N_4 phase

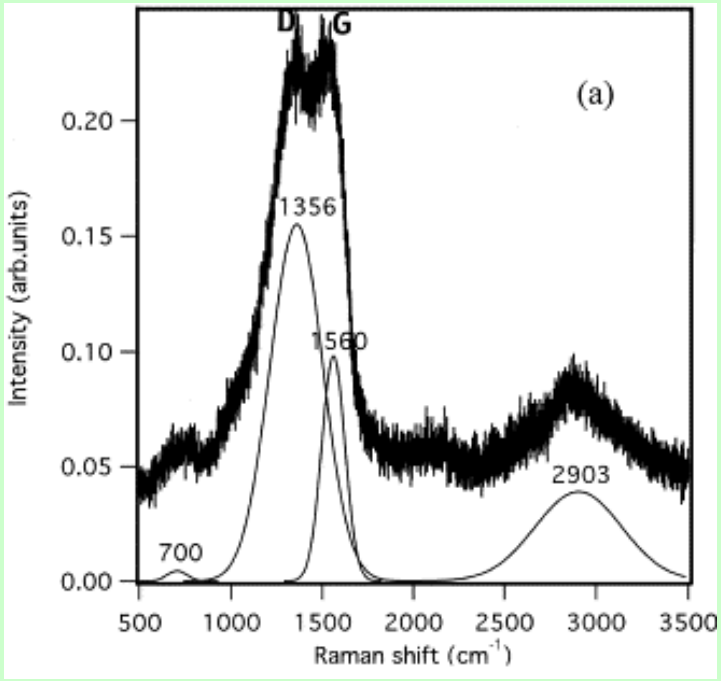

Raman spectrum of g-C_3N_4 (514 nm) From Andreyev, Akaishi, *Diam. Relat. Mater*. **11** 1885 (2002)

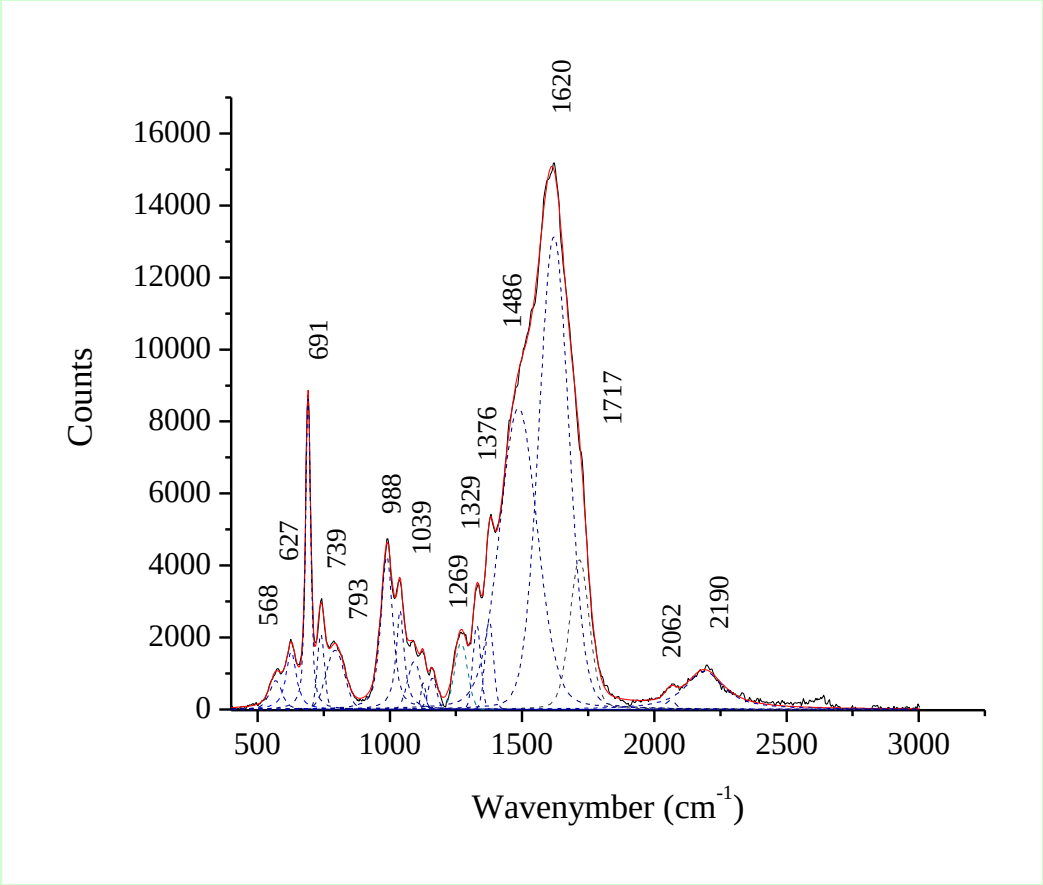

UV Raman (244 nm) spectrum of g-C_3N_4.

9:04 AM

Tentative assignment of the Raman peaks of *g*-C_3N_4 phase

The most prominent feature found on the UV Raman spectra of *g*-C3N4 is a sharp peak at 691(28) cm^{-1}. The next strongest peak is a peak centered at 988 (37) cm^{-1}. Appearance of two strong modes at 691 cm^{-1} and 988 cm^{-1} modes is unusual for graphitic phases such as graphite, hexagonal BN (*h*-BN), graphitic BCx phases.

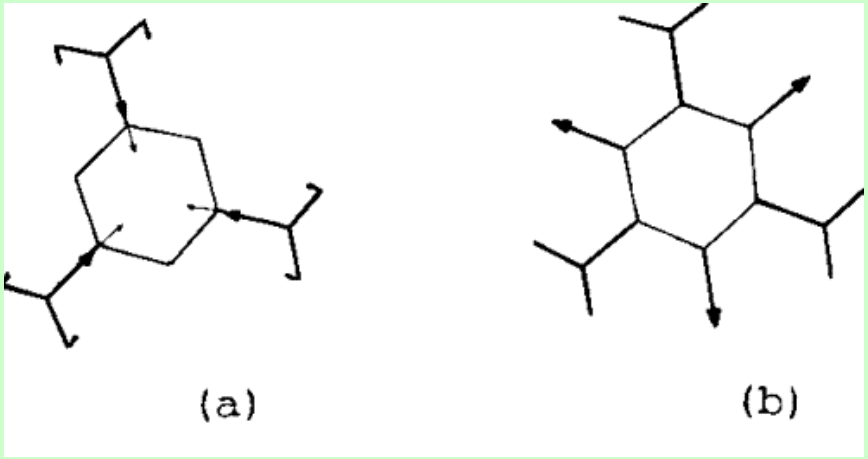

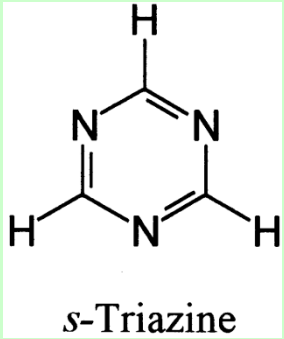

s-Triazine

The origin of the peak at 691 cm^{-1} and 988 cm^{-1} is related to the ring breathing vibration of the *s*-triazine rings (C_3N_3) inside *g*-C_3N_4 phase
Meier *et al*, *J. Phys. Chem.* **99** 5445 (1995).

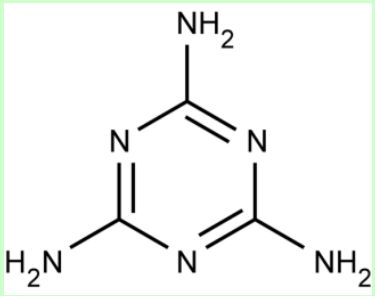

Melanime

9:04 AM

Home work

1. Give a definition of the confocal optical (Kentaro) and Raman (Shoko) microscopes.

2. Describe the difference in the image formation in reflection and transmission confocal microscopes (Kentaro).

3. Describe Raman spectra of graphite and diamond (Shoko).


Mahalo